Stony Brook University

Clathrin-Independent Endocytosis of ErbB2 in Human Breast Cancer Cells

A Dissertation Presented

By

Daniel John Barr

To

The Graduate School

In Partial Fulfillment of the

Requirements

For the Degree of

Doctor of Philosophy

In

Molecular and Cellular Biology

Stony Brook University

December 2007

Stony Brook University

The Graduate School

Daniel John Barr

We, the dissertation committee for the above candidate for the Doctor of Philosophy degree, hereby recommend acceptance of this dissertation.

Deborah A. Brown, Ph.D. – Dissertation Advisor
Professor, Department of Biochemistry and Cell Biology,
Stony Brook University

Erwin London, Ph.D. – Chairperson of Defense
Professor, Department of Biochemistry and Cell Biology,
Stony Brook University.

Simon Halegoua, Ph.D.
Professor, Department of Neurobiology and Behavior,
Stony Brook University

Jeffrey E. Pessin, Ph.D.
Professor, Department of Pharmacological Sciences
Stony Brook University

Nicole S. Sampson, Ph.D.
Professor, Department of Chemistry
Stony Brook University

This dissertation is accepted by the Graduate School

Lawrence Martin
Dean of the Graduate School

Abstract of the Dissertation

Clathrin–Independent Endocytosis of ErbB2 in Human Breast Cancer Cells

By

Daniel John Barr

Doctor of Philosophy

In

Molecular and Cellular Biology

Stony Brook University

2007

Endocytosis is an essential process required for functions including nutrient uptake, membrane recycling, and signal transduction. In comparison to the clathrin mediated pathway, clathrin-independent pathways are poorly understood. New work is beginning to reveal a picture of multiple non-clathrin pathways, including an Arf6 associated pathway and a pathway leading to GPI-anchored protein enriched early endosomes (GEECs).

The EGF receptor family member ErbB2 is overexpressed in 25-30% of human breast cancers. While ErbB2 is normally highly concentrated on the cell surface, the ansamycin antibiotic geldanamycin induces ubiquitination, internalization and degradation of the receptor. Here, we demonstrated that ErbB2 was internalized through a non-clathrin pathway in geldanamycin-treated SKBr3 human breast cancer cells. Internalization was not inhibited by dominant negative forms of Eps15 or dynamin, or by the clathrin inhibitor chlorpromazine. ErbB2 did not colocalize with transferrin or clathrin during initial internalization.

ErbB2 internalization did not require tyrosine kinase activity and did not occur by caveolae as SKBr3 cells lack detectable caveolae. The receptor colocalized with cholera toxin, a GPI-anchored protein and a fluid tracer, and was often found in ring shaped or tubular structures consistent with features of the GEEC pathway. The GEEC pathway was first described in Chinese Hamster Ovary (CHO) cells and thought to be specific for GPI-anchored proteins. We found that ErbB2 colocalized with GPI-anchored proteins Thy1 and PLAP soon after internalization in CHO cells. Surprisingly, ErbB2 and Thy1 also colocalized substantially with chimeric fusion proteins of PLAP containing transmembrane and cytosolic domains, proteins expected to be excluded from the GEEC pathway. Combined with other data from the lab, these results suggest that this pathway is not specific for GPI-anchored proteins, but may instead represent a bulk internalization pathway.

After internalization, ErbB2 was transported to the interior of early endosomes and then to late endosomes and lysosomes. Chloroquine retarded degradation of a truncated form of ErbB2. ErbB2 accumulated in vesicles containing constitutively-active Arf6Q67L only in the absence of geldanamycin. In geldanamycin-treated cells expressing Arf6Q67L, ErbB2 was transported to early and late endosomes, and degraded at the same rate as in untransfected cells.

Table of Contents

Abbreviations

AF	Alexa-Fluor
CELISA	Cell based enzyme linked immunosorbant assay
CHO	Chinese hamster ovary cells
CME	Clathrin mediated endocytosis
CCP	Clathrin coated pit
CCV	Clathrin coated vesicle
CLIC	Clathrin independent carrier
CPZ	Chlorpromazine
CQ	Chloroquine
CTxB	Cholera toxin B subunit
DN	Dominant negative
DRM	Detergent resistant membranes
EGFR	Epidermal growth factor receptor
Fl-Anti-ErbB2	Fluorescein-conjugated anti-ErbB2 antibodies
GA	Geldanamycin
GEEC	GPI-anchored protein enriched early endosome
GPI	Glycosyl phosphatidylinositol
IF	Immunofluorescence microscopy
PLAP	Placental alkaline phosphatase
PBS	Phosphate buffered saline
Rh-Tf	Rhodamine-conjugated Tf
SDS-PAGE	Sodium dodecyl polyacrylamide gel electrophoresis
Tf	Transferrin

List of Figures

Acknowledgements

I would like to start by thanking my graduate advisor, Dr. Deborah A. Brown. Debbie was kind enough to offer me a position in her lab and has been an excellent mentor. She has taught me is how to think independently and to persevere. Debbie's enthusiasm about science and the zeal with which she pursues research are contagious and have motivated me to work harder in the lab.

I would like to thank my committee members for all of the support and advice they have given me over the past five years. I would especially like to extend my gratitude to Dr. Erwin London who has offered me help and guidance from the day I started graduate school.

I would like to thank all of the members of the Brown lab. Many of the experiments in this dissertation would not have been possible without the help of Anne Ostermeyer-Faye. In addition to being a good friend Anne is a walking textbook for protocols and lab information. Special thanks to Dr. Laura Listenberger who has provided lots advice and encouragement. To the graduate students Prakhar Verma and Azad Gucwa thank you for making the lab environment a fun place to be. Special thanks to former lab member Rachel Matundan for her contribution to the Arf6 experiments.

I would like to thank my Good friends Peter Alff, Joseph Janda, and Lorenzo Bombardelli who have shared all the ups and downs of graduate school with me over the past 5 years.

I would like to thank my parents who have always offered encouragement and support.

Finally, I would like to thank Shivanjali Joshi, who is the most kind and caring person I have ever known and has always supported me.

Chapter 1. Introduction

Endocytosis is an essential cellular process where particles from the extracellular environment are brought inside the cells by the invagination and pinching off of a piece of plasma membrane. This process has historically been divided into two categories based on size: phagocytosis (or cell eating) and pinocytosis, (or cell drinking). Phagocytosis is mostly restricted to specialized mammalian cells such as macrophages, neutrophils, monocytes, and dendritic cells. It is an active and highly regulated process that requires actin reorganization and is regulated by Rho family GTPases. This pathway is specialized for the clearance and destruction of large pathogens such as bacteria or yeast, or other large debris such as fragments of dead cells (Aderem and Underhill, 1999). Pinocytosis on the other hand is a process that occurs in all cell types and is mechanistically diverse and highly regulated. This category encompasses clathrin mediated endocytosis, macropinocytosis, caveolae mediated endocytosis, and an emerging group of clathrin- and caveolar- independent pathways. They function in diverse processes such as nutrient uptake, signal transduction and maintenance of cellular homeostasis (Conner and Schmid, 2003). Work in this dissertation demonstrates that the receptor tyrosine kinase ErbB2 is internalized through a clathrin-independent pathway and adds to the expanding body of knowledge about clathrin independent pathways. This section

will introduce the different types of pinocytosis and the receptor tyrosine kinase ErbB2.

Clathrin Mediated Endocytosis

Clathrin mediated endocytosis (CME) is the best studied endocytic pathway. In most animal cell types the uptake of a major fraction of receptor-bound ligands and extracellular fluid results from the formation of clathrin-coated vesicles (CCVs) (Mellman, 1996). The defining feature of CME is a specialized protein coat composed of polyhedral lattices of clathrin that are assembled on the cytoplasmic leaflet of the plasma membrane. Clathrin coat formation induces the formation of an invagination called a clathrin coated pit (CCP), and following pinching off from the plasma membrane a CCV. The formation of the CCV is a multi-step process, orchestrated by many cellular proteins in a highly regulated manner (Brodsky *et al.*, 2001). Clathrin coated pits on the plasma membrane form first by the recruitment of soluble clathrin to the plasma membrane where it assembles into a latticework and forms a cage-like structure. The basic clathrin unit is composed of three copies of clathrin heavy chain and three copies of clathrin light chain that combine to form a 3 legged structure called a triskelion (Mellman, 1996).

Accessory proteins are required for assembly of the clathrin cage. Well studied examples are the monomeric assembly protein AP180, and the tetrameric

adaptor complexes, or APs. While AP180 expression is restricted to neuronal cells, an isoform named CALM (clathrin-assembly lymphoid-myeloid leukemia) is expressed ubiquitously. There are four related AP complexes, (AP1-4). However only AP-2 functions in clathrin coated vesicle formation from the plasma membrane (Kirchhausen, 1999).

CME occurs constitutively in mammalian cells. It functions in nutrient uptake, such as internalization of cholesterol containing low density lipoprotein (LDL) and iron bound to the blood protein transferrin (Tf) (Schmid, 1997; Brodsky *et al.*, 2001). CME also plays a major role in modulating signal transduction by both controlling the levels of cell surface receptor, and by removal of activated signaling receptors as a method of signal attenuation (Conner and Schmid, 2003). Although clathrin mediated endocytosis is a constitutive process, it is also highly selective. The recruitment of transmembrane proteins into coated pits requires binding of specific sorting sequences in the cytoplasmic domains to coat associated proteins. A common motif is the dileucine motif, or LL motif that is directly recognized by adaptor complex AP-2 (Aridor and Traub, 2002; Traub, 2003). Many coated pit motifs have been identified including the NPXY motif found in the tail of the LDL receptor, and the YPPΦ motif, variations of which are found in the transferrin receptor and the EGF receptor (Kirchhausen, 1999).

Once a clathrin coated pit has formed and cargo has been recruited to this nascent plasma membrane structure a mechanism must by in place to pinch off, or separate a vesicle from the plasma membrane. The GTPase dynamin serves this function. Dynamin is an unusually large GTPase containing multiple domains including a plecstrin homology domain, the GTPase effector domain, GTPase domain, a proline-rich domain, and a domain that functions as its own GTPase activating protein (GAP). The protein self-assembles into helical rings and stacks and is thought form a collar at the neck of a clathrin coated invagination (Sever *et al.*, 2000). Localization of this protein to clathrin coated pits is required for the scission and formation of clathrin coated vesicles. However, the exact function of this protein is not known. Two models have been proposed to explain dynamin action. One model suggests that dynamin functions as a mechanochemical enzyme and the conformational change resulting from GTP hydrolysis drives the enzyme to constrict around the neck of a coated pit severing it from the membrane (Hinshaw and Schmid, 1995; Sweitzer and Hinshaw, 1998). An alternate model suggests that dynamin plays a regulatory role and like other GTPases functions to recruit downstream effectors (Sever *et al.*, 1999). Dynamin, in addition to its important function in CME is also required for phagocytosis, caveolae mediated endocytosis, and some clathrin independent pathways.

Once the clathrin coated vesicle is severed from the membrane these vesicles lose their clathrin coat and acquire the small GTPase Rab5. The newly

internalized vesicles then merge with early sorting endosomes in a process that requires Rab5 activity. Cargo delivered to the early endosome is sorted and sent to its ultimate destination. Some examples of cargoes that traffic to different locations are discussed below.

The transferrin receptor is a well studied clathrin cargo. Internalization is constitutive, and the receptor is concentrated in clathrin coated pits by recognition of the sorting sequence in the cytoplasmic tail. It is rapidly internalized with a half life of 2 minutes and delivered to the early sorting endosomes. From there it is transported to vesicular-tubular recycling compartment where is it returned to the plasma membrane (Maxfield and McGraw, 2004). Many clathrin cargos are internalized and recycled like the transferrin receptor. Other receptors are destined for a different fate.

The EGF receptor is another well studied clathrin cargo that is internalized after binding EGF. Ligand binding results in rapid internalization through CME in a process that requires both the growth factor binding protein Grb2, and ubiquitination of activated EGFR by the E3 ubiquitin ligase c-Cbl (Wang and Moran, 1996; Duan *et al.*, 2003; de Melker *et al.*, 2004a). Receptor internalization in this case results in trafficking through early endosomes to late endosomes, and ultimately to lysosomes where the receptor is degraded (Stern *et al.*, 1986; King *et al.*, 1988; Lenferink *et al.*, 1998). It is important to note however, that EGF receptor is exclusively internalized through CME at low,

physiological concentrations of EGF. At higher ligand concentration the clathrin mediated pathway is saturable and EGF receptor may be internalized by other clathrin-independent mechanisms (Lund *et al.*, 1990; Jiang *et al.*, 2003).

Clathrin- Independent Endocytic Pathways

The process of macropinocytosis and caveolar endocytosis are two highly regulated processes that operate independently of clathrin. These pathways are described below. Clathrin-independent pathways distinct from macropinocytosis and caveolar endocytosis have also been described. These are categorized below as clathrin- and caveolin-independent endocytosis and further divided into classes based on the requirement for dynamin.

Macropinocytosis

Macropinocytosis is an actin dependent process that is regulated by the Rho family GTPase Rac1. Actin polymerization drives the formation of membrane ruffles and protrusions that collapse back onto and fuse with the plasma membrane. This process generates large endocytic vesicles of variable size called macropinosomes that contain large volumes of fluid. The mechanics behind this highly regulated process are not well understood.

Macropinocytosis can be induced transiently in many cell types and performs diverse functions (Cardelli, 2001). For example activation of dendritic cells leads to a prolonged burst of macropinocytic activity that functions in immune surveillance (Mellman and Steinman, 2001). Growth factor induced macropinocytosis may play a role in directed cell migration (Ridley, 2001). Additionally, some bacteria such as Salmonella inject toxins into cells that can activate Rho family GTPases and induce macropinocytosis (Hueffer and Galan, 2004). These bacteria are then taken into the cell by this mechanism where they can form a replicative niche (Steele-Mortimer *et al.*, 2000). Specific inhibitors of macropinocytosis are derivatives of amiloride, a drug that blocks Na+/H+ exchange, but these reagents may also inhibit other uptake mechanisms (Meier *et al.*, 2002; Wadia *et al.*, 2004).

Caveolar Endocytosis

Caveolae were first identified over 50 years ago as uncoated, flask shaped invaginations on the plasma membrane (Yamada, 1955) . Although the discovery of caveolae predates the identification of clathrin coated pits by ten years, our understanding of the function of these unique organelles is just emerging (Parton and Simons, 2007). Caveolae are highly abundant and present in most cell types. They demarcate lipid rafts, or domains in plasma membrane domains enriched in cholesterol and sphingolipids (Anderson, 1998; Kurzchalia and Parton, 1999).

Caveolins, a group of oligomeric cholesterol binding proteins that insert into the membrane as a hairpin loop are the major protein constituent of caveolae (Rothberg *et al.*, 1992; Dupree *et al.*, 1993; Monier *et al.*, 1995). Caveolins 1-3 make up the caveolin family. Of these caveolin-3 expression is restricted to muscle cells, while caveolin 1 and 2 are abundant in most other cell types (Way and Parton, 1995; Tang *et al.*, 1996). Caveolin-1 and caveolin-3 are essential for caveolae formation, while caveolin-2 has no apparent effect (Drab *et al.*, 2001; Galbiati *et al.*, 2001). Lymphocytes normally lack caveolae and the expression of caveolin-1. Exogenous expression of caveolin-1 in these cells was enough to drive caveolae formation (Fra *et al.*, 1995).

The biological role for caveolae remains hotly debated. These organelles a have been implicated in regulation of signal transduction, maintenance of cholesterol homeostasis, and endocytosis (Razani *et al.*, 2002; Parton and Simons, 2007). In support of a role for caveolae regulating signal transduction many signaling molecules are concentrated in caveolae. This points to a function in compartmentalization and regulation of signaling cascades (Anderson, 1998). Additionally, caveolin-1 knock-out mice, while having no overt phenotype, show hyperproliferative response in the lung endothelia and other tissues (Razani *et al.*, 2001). However, since caveolin-1 null mice develop normally and are not more susceptible to tumors than wild type mice a broader role as a negative regulator of signaling pathways is unlikely. Caveolae also play a role in endocytosis although

several studies now suggest that caveolae function in endocytosis is more complicated then previously thought.

Caveolae are stable structures at the plasma membrane. Fluorescence recovery after photobleaching (FRAP) showed that caveolae structures are stationary; they exhibit little lateral movement in the membrane and are not constitutively internalized (Pelkmans *et al.*, 2002; Thomsen *et al.*, 2002). Caveolae endocytosis instead is regulated and must be triggered by phosphorylation of caveolin-1 (Minshall *et al.*, 2000). Experimentally, this can be achieved by treatment of cells with phosphatase inhibitors such as okadaic acid (Parton *et al.*, 1994). Beside a requirement for phosphorylation caveolar endocytosis requires dynamin activity, actin polymerization and membrane cholesterol.

Caveolae are endocytic carriers of albumin in the process of transcytosis (Schubert *et al.*, 2001) . Serum albumin binds to the serum albumin receptor gp60, a receptor concentrated in caveolae (Tiruppathi *et al.*, 1997). Albumin binding results in a Src dependent phosphorylation of caveolae, and transcytosis of albumin (Minshall *et al.*, 2000). Endothelial cells that lack caveolin-1 are unable to bind and internalize albumin, although in knock-out mice there is no defect in albumin transcytosis. This highlights the possible existence of redundant mechanisms in mice. Cross-linked GPI-anchored proteins, the TGF-B receptor, and toxins or pathogens such as cholera toxin and SV40 virus have been

reported as caveolar cargos (Pelkmans and Helenius, 2002; Di Guglielmo *et al.*, 2003; Pelkmans, 2005). Studies with SV40 virus have perhaps been the most illuminating. This virus binds the ganglioside GM1 as its receptor and is internalized by caveolae (Pelkmans *et al.*, 2001; Campanero-Rhodes *et al.*, 2007). Once SV40 virus binds its receptor, the virus is rapidly sequestered in caveolae, and internalized in a process requiring tyrosine kinase activity, dynamin recruitment, and local actin reorganization (Pelkmans *et al.*, 2002). The virus is then transported to a preexisting caveolin-1 containing organelle devoid of clathrin cargos and markers of early endosomes (Pelkmans *et al.*, 2001). The term "caveosome" was coined for this novel organelle, and SV40 is then sorted from this structure and transported to the endoplasmic reticulum in a microtubule dependent manner where the virus can establish a productive infection (Pelkmans *et al.*, 2001). Studies with SV40 virus also serve to showcase many uncertainties behind caveolar endocytosis. In particular, later studies showed that SV40 can also be internalized and establish a productive infection in cells devoid of caveolae (Damm *et al.*, 2005). Viral uptake in caveolin-1 null cells resembles infection in caveolin-1 expressing cells in that tyrosine kinase activity is required, and the virus is transported to structures resembling caveosomes. They differ in that SV40 virus uptake in caveolin-1 null cells does not require dynamin recruitment, and the kinetics of internalization are faster(Pelkmans *et al.*, 2004; Damm *et al.*, 2005). This raises the question of whether the same pathway

operates in both cell types, and whether caveolin-1 is a dispensable component. It is now clear that caveolar endocytosis represents a major pathway of entry for some viral pathogens. However, the physiological importance of this highly regulated pathway is not yet understood.

Clathrin- and Caveolar-Independent Endocytic Pathways

Clathrin- and caveolar-independent pathways represent a rapidly evolving field of study. Compared to the clathrin mediated pathway, the molecular details of how vesicles are formed and how these pathways are regulated are not well understood (Conner and Schmid, 2003). This is best illustrated by the fact that that these pathways are almost always described in negative terms. Advancements in our understanding of these pathways come primarily from identification of cargo molecules internalized through non-clathrin pathways and identification of possible regulators (Mayor and Pagano, 2007). However, this has led to confusion about how many of these clathrin independent pathways exist, and how they may overlap mechanistically and functionally. Adding to the confusion is the fact that many cargos can be internalized through multiple pathways. This is perhaps best illustrated by cholera toxin, a promiscuous cargo that can be taken up by CME, caveolar endocytosis, and other pathways (Massol *et al.*, 2004).

Clathrin- independent pathways can first be categorized based on a requirement for the large GTPase dynamin (Mayor and Pagano, 2007). Aside from the caveolar pathway described earlier, only one other clathrin independent pathway has been identified that requires dynamin. This pathway was uncovered while studying the internalization of the β subunit of the IL-2 receptor. The IL-2 receptor is expressed in lymphoid cells, and some non-lymphoid cell types including fibroblasts, endothelial, epithelial, and neuronal cell. Activation of the receptor occurs after IL-2 binding; the receptor is then efficiently internalized and targeted for degradation in lysosomes. Work on this receptor determined that it was not recruited into clathrin coated pits, and further, expression of dominant negative isoforms of proteins required for CME (Eps15; cAP180) did not block its internalization. The receptor is associated with detergent resistant membranes (DRMs), a salient trait of many clathrin independent cargos. Additionally, internalization of this receptor in lymphoid cells required the GTPase RhoA (Lamaze *et al.*, 2001). Dynamin- independent pathways include a pathway leading to novel structures called GPI-anchored protein enriched early endosomes (GEECs), termed the GEEC pathway, and an endocytic pathway associated with the small GTPase Arf6 (Sabharanjak *et al.*, 2002; Naslavsky *et al.*, 2004; Kalia *et al.*, 2006). Features and cargos of these different pathways will be described in detail next.

Dynamin- Independent Non- Clathrin Pathways

Much confusion in the literature revolves around the dynamin independent non-clathrin pathways. In particular, the pathways resemble one another in the types of cargos that are internalized, but differ regarding the GTPases that regulate these pathways. Apparently, cell type difference may also exist (Kalia *et al.*, 2006). Two pinocytic pathways that have been described recently are the GEEC pathway and the Arf6 associated pathway.

The GEEC Pathway

The GEEC pathway was characterized in Chinese hamster ovary cells (CHO), and first reported by Mayor and colleagues in 2002. They found that after a short internalization time, GPI-anchored proteins were found in vesicles devoid of markers for the clathrin pathway. These vesicles did not contain Rab5, were enriched in GPI-anchored proteins, and contained detectable amounts of a fluid phase marker. Due to their enrichment in GPI-anchored proteins, these compartments were named GPI-anchored protein enriched endosomal compartments, or GEECS. Endocytosis to this compartment was specific for GPI-anchored proteins, as chimeric proteins containing the extracellular domain of a GPI-anchored protein fused a transmembrane domain were excluded. When cells were treated with *Clostridium difficile* Toxin B, which irreversibly inactivates Rho family GTPases by glucosylation, fluid phase uptake was

blocked. Expression of dominant negative isoforms of RhoA, Rac1, or cdc42 revealed that cdc42 function was necessary for fluid phase uptake. Surprisingly, though, Toxin B treatment did not affect the extent of GPI-anchored protein internalization. This suggested that loss of cdc4 function might lead to internalization of GPI-anchored proteins by a different pathway. To test this idea, the authors examined the localization of a GPI-anchored protein and transferrin in control and DN cdc42-expressing cells. They found that after 2 minutes of internalization, there was significantly more colocalization of Tf with the GPI-anchored protein in DN cdc42 expressing cells than in control cells expressing wild-type cdc42. They concluded that that cdc42 regulates the GEEC pathway, and that inactivation of cdc42 results in a redirection of GPI-anchored proteins into the clathrin mediated pathway.

Further work in mouse embryonic fibroblasts using an ultrastructural electron microscopy assay has revealed morphological details about the structure of the initial endocytic carriers (Kirkham *et al.*, 2005). These were initially named CLICs for Clathrin Independent Carriers, but are now recognized as corresponding to GEECs. These structures were tubular, or ring shaped with average diameters between 40-80nm. In addition for being the bulk internalization route for GPI-anchored proteins and fluid, this pathway also represents the major route for cholera toxin uptake. GEECs/CLICs eventually acquire Rab5 in a PI3

kinase dependent manner and then fuse with early endosomes, where GEEC cargos merge with cargos taken up by the clathrin pathway.

Arf6 Associated Pathway

In contrast to the GEEC pathway, much of the work describing the Arf6 pathway has been done in Hela cells. Arf6 is a member of the Arf family of small GTPases, and a member of the Ras superfamily. Proteins in the Arf family are thought to function by regulating the recruitment of cytosolic coat proteins onto membranes to facilitate sorting and vesicle formation, by the activation of lipid modifying enzymes, and through the modulation of actin structures (Donaldson, 2003). Cargos internalized through the Arf6 associated pathway are major histocompatability complex 1 (MHC1), the GPI-anchored protein CD59, and the IL-2 receptor alpha subunit (Tac) (Naslavsky *et al.*, 2004). Internalization of these proteins is dynamin independent and the proteins are found in Arf6 decorated vesicles that are devoid of clathrin cargos. Arf6 positive vesicles ultimately merge with early endosomes containing cargo from the clathrin mediated pathway in a process requiring Arf6 inactivation. Expression of a constitutively active Arf6 isoform resulted in entrapment of clathrin independent cargos in enlarged, Arf6 labeled compartments. Similarly, fusion of Arf6 compartments with early endosomes can be prevented by treatment with wortmannin or Ly294002, drugs that inhibit PI3 kinase activity (Naslavsky *et al.*,

2003). Along with inactivation of Arf6, changes in phosphoinositide from phosphoinositide-2-phosphate (PI2P) to phosphoinositide bis-phosphate (PI3P), modulated by PI3kinase, are required for recruitment of EEA1 and Rab5 onto Arf6 positive endosomes. This event is required for fusion with early endosomes that contain clathrin cargos such as the LDL receptor.

Importantly, cells expressing constitutively active Arf6 exhibit a two-fold stimulation in internalization. Furthermore, as discussed earlier, cargos become trapped in enlarged endosomes (Naslavsky *et al.*, 2004). Expression of a dominant negative isoform of Arf6 results in a very slight decrease in internalization. The mild effect of dominant negative Arf6 suggests that the Arf6 activity is not required for internalization. While the protein has obvious important functions during the early stages of trafficking clathrin independent cargos a direct role for Arf6 in internalization has not yet been established.

The GEEC pathway and the Arf6-associated pathway share common features in that GPI-anchored proteins can be internalized through both pathways, and that cargo from these pathways eventually merges with clathrin derived cargos in a process requiring PI3 kinase. For both pathways, the mechanics of vesicle formation and scission from the plasma membrane remain poorly understood. A consequence of this is that both pathways are named after characteristics of the earliest known endocytic compartment in this pathway and not after the internalization mechanism. Both of these pathways appear to be

constitutive and function as bulk endocytic pathways. While the pathways share several similarities, differences seems to be largely cell type specific. In contrast to Arf6 studies in HeLa cells, endogenous Arf6 labeled transferrin containing endosomes soon after internalization in CHO cells (Kalia *et al.*, 2006). While cell type specific differences clearly exist between these two pathways the relationship between these two pathways is not entirely clear.

The ErbB Family of Receptor Tyrosine Kinases

The focus of this study is the endocytic pathway followed by the ErbB receptor family member ErbB2 upon destabilization with geldanamycin (GA). The next sections will describe this family and how ErbB2 is targeted for internalization and degradation

The ErbB family of receptor tyrosine kinases constitutes one of the most studied groups of cell surface receptors. Proteins of this family couple the binding of extracellular growth factor ligands to intracellular signaling pathways. They are widely expressed in epithelial, mesenchymal and neuronal tissues and regulate a diverse array of signaling responses, including proliferation, differentiation, motility, and cell survival signals (Rowinsky, 2004). This family includes four structurally related members; ErbB1 or the epidermal growth factor (EGF) receptor, ErbB2, ErbB3, and ErbB4. Structurally, members of this family share two cysteine-rich extracellular domains involved in ligand binding, an a

intracellular kinase domain, and a carboxy-terminal tail containing autophosphorylation sites (Yarden and Sliwkowski, 2001). Members of the ErbB family bind 20 or more different ligands. Ligand binding results in receptor dimerization and cross phosphorylation. Members of this receptor family are capable of forming homo- and heterodimers. The cellular outcome of ErbB activation as well as the magnitude of signal induced are dependent on the composition of the dimer pair and the identity of the ligand (Yarden and Sliwkowski, 2001). This receptor family is of considerable clinical interest due to their frequent involvement in human cancers. Of these, The EGF receptor and ErbB2 are most frequently involved with human malignancies (Roskoski, 2004).

ErbB2

ErbB2, also called Her-2 is unique among other EGF family members in that it has no known ligand (Citri *et al.*, 2003). Instead under normal conditions the receptor signals by heterodimerizing with other ErbB family members after they bind ligand (Citri *et al.*, 2004). ErbB2 is the favored heterodimer partner for the other ErbB proteins. Dimerization is mediated by a unique dimerization arm localized to the extracellular (N terminal) portion of the receptor. Whereas exposure of this arm normally requires ligand binding and reorganization of the exterior portion of ErbB receptors, it is constitutively exposed in ErbB2 (Burgess *et al.*, 2003; Garrett *et al.*, 2003). ErbB2 containing complexes form extremely

potent signaling modules. Homodimers formed from EGF receptor alone, or heterodimers formed from EGF receptor and ErbB4 form comparatively weak signaling complexes compared to heterodimers containing ErbB2. An extremely active signaling module is formed from ErbB2 and ErbB3. Alone, each of these receptors is signaling incompetent as ErbB2 lacks a ligand and ErbB3 has no kinase activity. However, paired together these form a strong signaling module (Citri *et al.*, 2003).

ErbB2 is overexpressed in 20-30% human breast cancers and is associated with poor prognosis (Slamon *et al.*, 1987). Thus ErbB2 has received intense clinical interest as a target for cancer therapies with ErbB2 downregulation as an important goal in these studies. Two experimental approaches for ErbB2 downregulation that have witnessed success are inhibitory monoclonal antibodies directed against ErbB2 and pharmacolological agents that induce ErbB2 degradation. The mouse chimeric humanized monoclonal antibody trastuzumab (Herceptin) was approved for treatment of ErbB2-expressing breast cancers in 1998 (Cobleigh *et al.*, 1999). Patients undergoing ErbB2 targeted cancer treatment are first screened for ErbB2 upregulation by fluorescence in situ hybridization, and trastuzumab is then administered intravenously alone or in combination with other anti-cancer agents (Roskoski, 2004). While antibody treatment has met with success, about 5% of patients receiving the treatment develop congestive heart failure; still others show no response to the treatment.

Often, many patients relapse after initially responding to treatment (Cobleigh *et al.*, 1999).

Pharmacological agents that downregulate ErbB2 are also being explored. Of these the benzoquinone ansamycin antibiotic geldanamycin (GA) and its derivatives show therapeutic promise. These agents induce Erbb2 degradation indirectly by acting on the heat shock protein hsp90, discussed in more detail below. The GA derivative 17-demethoxygeldanamycin (17-AAG, NSC 330507) is under clinical development (Sharp and Workman, 2006).

Unlike other EGF family proteins, ErbB2 is found in a constitutive complex with the heat shock protein hsp90 (Xu *et al.*, 2001). Hsp90 binds to a loop in the kinase domain of ErbB2 and restrains ErbB2 activity. Heterodimerization displaces hsp90 and activates ErbB2 by a Src dependent mechanism (Xu *et al.*, 2007). Displacement of hsp90 also destabilizes ErbB2, as is true for other hsp90 client proteins (Hohfeld *et al.*, 2001; Richter and Buchner, 2001). GA disrupts hsp90 interaction with ErbB2 by binding to the ATP binding site of hsp90 locking the protein in the ADP bound conformation and preventing its interaction with ErbB2 (Xu *et al.*, 2001). Following release of hsp90 from ErbB2 the chaperone hsp70 and its co-chaperone and E3 ubiquitin ligase CHIP are recruited to the receptor. CHIP ubiquitinates ErbB2 leading to its degradation in lysosomes with a half time of 2 hours (Xu *et al.*, 2002; Zhou *et al.*, 2003; Citri *et al.*, 2004).

Early reports suggested that after release of Hsp90, ErbB2 is degraded by proteasomes, rather than in lysosomes (Mimnaugh *et al.*, 1996; Citri *et al.*, 2002; Way *et al.*, 2004). However, recent data suggest that the protein is transported through early and late endosomes for degradation in lysosomes. Internalized ErbB2 colocalizes with transferrin (Tf), and is present in internal vesicles inside multivesicular bodies (MVBs), suggesting transport to lysosomes for degradation (Austin *et al.*, 2004). Surprisingly, though, these authors found little colocalization of ErbB2 with markers of late endosomes or lysosomes (Austin *et al.*, 2004).

ErbB2 degradation was initially reported to be insensitive to lysosomal inhibitors (Mimnaugh *et al.*, 1996; Citri *et al.*, 2002; Way *et al.*, 2004). However, later work showed that a 23 kDa cytoplasmic domain fragment is cleaved from Erb2 in GA-treated cells in a caspase dependent manner. Previous studies used an antibody directed against the 23kDa cytosolic cleavage product, rendering the protein undetectable by Western blotting (Tikhomirov and Carpenter, 2000, , 2001). Use of an extracellular domain-specific antibody showed that lysosomal inhibitors stabilize a clipped 135 kDa form of ErbB2 in GA-treated cells (Tikhomirov and Carpenter, 2000). Another study showed that proteasome inhibitors retard ErbB2 degradation in GA-treated cells indirectly, by inhibiting internalization, and that even intact ErbB2 can be internalized and degraded in lysosomes upon GA treatment (Lerdrup *et al.*, 2006)

While it is now clear that GA action leads to degradation of ErbB2 in lysosomes, whether GA induces ErbB2 internalization remains controversial. Two models have emerged to explain the endocytic status of ErbB2. One model favored by Hommelgaard and colleagues described ErbB2 as an internalization resistant receptor that is static on the cell surface (Hommelgaard *et al.*, 2004). GA treatment of cells induces degradation of the receptor by causing it to be internalized by an unknown mechanism; the receptor is then targeted to lysosomes for destruction. These workers showed that ErbB2 is preferentially associated with membrane protrusions, is efficiently excluded from clathrin coated pits (CCP), and is not found in internal structures. Furthermore they showed that receptor localization to protrusions does not change after binding of the Herceptin antibody, or EGF. ErbB2 redistribution required extensive crosslinking to free the antibody from membrane protrusions (Hommelgaard *et al.*, 2004). Another report used fluorescence recovery after photobleaching (FRAP) to show that GA treatment caused a significant increase in the amount of mobile ErbB2 in the plasma membrane compared to untreated cells (Lerdrup *et al.*, 2006). Following the initial internalization step ErbB2 was transported to early endosomes, late endosomes, and ultimately lysosomes where the protein was degraded. In summary, this data from these reports suggest that ErbB2 is normally an internalization-resistant receptor that localizes to membrane

protrusions, and that GA induces increased plasma membrane mobility and endocytosis of the receptor.

In contrast, another model describes the status of ErbB2 as mobile and capable of being internalized continuously. At a steady state Erbb2 is internalized and then rapidly recycled back to the plasma membrane (Austin *et al.*, 2004). According to this model, GA-induced ubiquitination is recognized in endosomes, where it redirects the cellular itinerary of ErbB2 from a recycling pathway to lysosomal transport. Studies using an assay that relied on quenching of extracellular bound antibody found that Herceptin did not influence the distribution of ErbB2 and instead recycled passively with the receptor. Additionally, internalized receptor colocalized with markers of the recycling pathway. Initial internalization kinetics were the same when the cells were treated with GA except now the receptor did not recycle and was instead sorted to lysosomes for degradation (Austin *et al.*, 2004).

ErbB2 has garnered a considerable amount of interest in recent years due to its frequent involvement in breast cancer. However, the precise mechanism by which the receptor is internalized and targeted for degradation is not known. While most workers now agree that GA treatment results in ErbB2 degradation in lysosomes, whether the protein is stably anchored at the plasma membrane, or whether it is constitutively internalized and recycled remains controversial. Additionally, no studies have been done to determine how ErbB2 is internalized.

As earlier workers saw very low amounts of ErbB2 in clathrin coated pits and did not see ErbB2 in transferrin-containing endosomes by electron microscopy, it seemed likely that ErbB2 is internalized by a clathrin-independent pathway (Hommelgaard *et al.*, 2004). However, another group did see an effect of clathrin inhibitors on ErbB2 internalization (Austin *et al.*, 2005). Data in this dissertation address ErbB2 endocytosis and, in contrast to the earlier report (2005) show that ErbB2 is internalized through a clathrin-independent pathway.

Chapter 2. Materials and Methods

Materials

Cells and Transfection

SKBr3 human breast cancer cells, from American Type Culture Collection (ATCC, Manassas, VA), were maintained in Dulbecco's modified Eagle's medium with 10% iron-supplemented calf serum (JRH, Lenexa, KS) and penicillin/streptomycin. Cells were transiently transfected with Lipofectamine 2000 (Invitrogen, Carlsbad, CA) according to the manufacturer's recommendation, and examined 1-2 days post-transfection, except for cells expressing Arf6-Q67L, which were examined 14-16 hours post-transfection.

Plasmids

A plasmid encoding the GFP-tagged Eps15 mutant ΔE95/295 (Benmerah *et al.*, 1999) was the gift of A. Benmerah (Institut Cochin, Paris, France). Tetracycline-inducible dominant negative (DN; K44A) HA-tagged dynamin-1 (Damke *et al.*, 1994) was the gift of J. Pessin (Stony Brook University School of Medicine, Stony Brook, NY). For maximal expression, this plasmid was co-expressed with pTet-Off, expressing a tetracycline-controlled transactivator (Clontech Laboratories Inc., Mountain View, CA). HA-tagged constitutively-active Arf6-Q67L (Hernandez-Deviez *et al.*, 2004) in pCB7 (Frank *et al.*, 1998) was the gift of J. Casanova (University of Virginia, Charlottesville, VA).

pBC12/PLAP and PLAP-G encoding placental alkaline phosphatase (Berger *et al.*, 1987) was the gift of Dr. S. Udenfriend (deceased). PLAP-HA was constructed as described (Arreaza and Brown, 1995). EGFP-tagged wild-type and constitutively-active (Q79L) Rab5 plasmids (Volpicelli *et al.*, 2001) were from Dr. A. Levey (Emory University School of Medicine, Atlanta GA). A GFP-tagged Rab7 plasmid (Guignot *et al.*, 2004) was the gift of Dr. C. Roy (Yale University School of Medicine, New Haven, CT).

Antibodies, Fluorescent Compounds, and Other Reagents

Anti-ErbB2 antibodies: for immunofluorescence microscopy (IF), monoclonal antibodies 4D5 (purified from supernatant of hybridoma cells (ATCC) grown in an Integra Biosciences CELLine two-compartment bioreactor, from Microbiology International (Frederick, MD)), or 9G6.10 or N28 (for acid-stripping experiments) from LabVision (Fremont, CA) were used for cell-surface detection. Rabbit polyclonal anti-ErbB2 antibodies (DakoCytomation USA, Carpinteria, CA) or the monoclonal antibodies listed above (as indicated) were used on fixed/permeabilized cells. LabVision anti-ErbB2 antibody #20 was used on blots. Monoclonal anti-epidermal growth factor receptor (EGFR) antibody #3 was from LabVision. Rabbit anti-clathrin heavy chain antibodies (Simpson *et al.*, 1996) were the gift of Dr. M. S. Robinson (University of Cambridge, Cambridge Institute of Medical Research, Cambridge, UK). Rabbit anti-HA tag antibodies

were from Santa Cruz Biotechnology (Santa Cruz, CA), and mouse monoclonal anti-HA tag antibodies were from Applied Biological Materials (Vancouver, BC, Canada). Mouse monoclonal anti-phosphotyrosine antibodies were from Upstate Biological (Lake Placid, NY). Anti-EEA1 antibodies were from Transduction Laboratories, BD Biosciences (San Jose, CA). Monoclonal anti-CD63 antibodies were from the Developmental Studies Hybridoma Bank, University of Iowa (Iowa City, IA). Rabbit anti-LAMP-1 antibodies were from Affinity Bioreagents (Golden, CO). Rabbit anti-PLAP antibodies were from DakoCytomation USA. Rabbit Anti-PLAP Fab fragments were prepared using immobilized papain on agarose beads (Pierce, Rockford, IL) according to instructions from the supplier. Mouse anti-PLAP antibodies Clone 8B6 were obtained from Labvision. Mouse anti-Thy1 antibodies were obtained from Transduction labs. Fluorescently labeled mouse anti-PLAP and anti-Thy1 Fab fragments were generated by first labeling whole antibody with Alexa-Fluor 488 (Anti-PLAP) or Alexa-Fluor-594 (Anti-Thy1) tetrafluorophenyl (TFP) reactive dyes according to the manufacturers guidelines (Invitrogen, Carlsbad, CA). Labeled whole antibody was then digested using Ficin immobilized on agarose beads following the supplier's instructions generate Fab fragments (Pierce, Rockford IL). Fluorescein was conjugated to anti-ErbB2 and anti-EGFR antibodies and to anti-PLAP Fab fragments, rhodamine to human transferrin (Tf), and biotin to anti-ErbB2 antibodies using N-hydroxysuccinimide-fluorescein or -rhodamine or -PEO_4-biotin (Pierce), using

conditions recommended by the supplier. Alexa Fluor (AF)-594-Tf was from Molecular Probes, Invitrogen (Carlsbad, CA). Secondary antibodies; dichlorotriazinylaminofluorescein-goat anti-mouse IgG, fluorescein-goat anti-rabbit IgG, Texas red-goat anti-mouse IgG, Texas red-goat anti-rabbit IgG, and horseradish peroxidase-goat anti-mouse IgG were from Jackson Immunoresearch Laboratories (West Grove, PA). AF-350-goat anti-mouse IgG and goat anti-rabbit IgG, AF-594-cholera toxin B subunit (AF-594-CTxB), AF-680-goat anti-mouse IgG and -goat anti-rabbit IgG used for fluorescent detection of bands on blots, and FluoroRuby^{TM} dextran (10,000 MW) were from Molecular Probes, Invitrogen. In the experiment shown in Fig. 1D,E, the AF-488 Zenon Mouse IgG labeling kit (Molecular Probes, Invitrogen), consisting of fluorescently-tagged goat anti-mouse Fab fragments, was used to detect anti-ErbB2 antibodies using conditions recommended by the supplier. Other Reagents: GA was from the Drug Synthesis and Chemistry Branch, National Cancer Institute (Bethesda, MD). EGF was from Calbiochem, EMD Biosciences (San Diego, CA). Human Tf, chlorpromazine (CPZ), chloroquine (CQ), genistein, peroxidase-conjugated streptavidin polymer, and other reagents were from Sigma Aldrich (St. Louis, MO).

Methods

Fluorescence microscopy

Cells were seeded on acid-washed glass coverslips, transfected (if appropriate) the next day, and examined 1-2 days after seeding or transfection. After drug treatment, antibody binding, and/or warming as described below and in the figure legends, cells were fixed with phosphate-buffered saline (PBS; 150 mM NaCl, 20 mM phosphate buffer, pH 7.4) containing 3% paraformaldehyde for 30 minutes, permeabilized at room temperature with PBS containing 0.5% Triton X-100 (except for detection of LAMP-1), and blocked with PBS containing 3% BSA and 10 mM glycine. For detection of LAMP-1, after fixation cells were permeabilized with PBS containing 0.5% saponin. Cells were then treated for 10 minutes at room temperature with PBS containing 0.1% sodium borohydride and 0.1% saponin, and then blocked and incubated with primary and secondary antibodies as described above, except that 0.1% saponin was included in all solutions. Images were captured and processed by epifluorescence microscopy as described (Ostermeyer *et al.*, 2001; Ostermeyer *et al.*, 2004) or by deconvolution microscopy using a Zeiss Axiovert 200 deconvolution microscope and processing images with Axiovision software (version 4.4). To acquire Z stacks, 25-35 serial images were recorded at 350 nm intervals along the Z axis using a 63x or 100x oil immersion objective. Out of plane fluorescence was removed by deconvolution using the inverse filter algorithm or a modification of the constrained iterative

algorithm. Images shown are representative sections from deconvolved Z- stacks or maximum intensity projections of Z stacks. Confocal image acquisition for colocalization analysis was performed on a Zeiss Pascal laser scanning confocal microscope. Images were acquired using 40x oil immersion objective. Airy units were set to 1 and levels for laser intensity and detector gain were optimized for each slide before image acquisition.

Except where indicated, cells were treated with 5 μM GA, for times indicated in figure legends. For internalization assays, surface-bound antibodies (2 μg/ml) were bound to cells at 4°C for 1 hour. For internalization times ≥30 minutes, cells were returned to a 37°C incubator. For internalization times ≤5 minutes, cells were then transferred to a 37°C water bath with a change to prewarmed media for the indicated times, and then washed with ice-cold PBS and transferred back to ice. To facilitate detection of internalized antibodies after short internalization times, residual surface-bound antibodies were stripped from cells with acid wash solution (100 mM Gly, 50 mM KCl, 20 mM magnesium acetate pH 2.3), using 3 washes of 3 minutes each. Fluorescent Tf (35 μg/ml) was either bound to cells together with antibodies, or was included in the media during warming, as indicated.

Colocalization Analysis

Quantification of colocalization was performed using imageJ software (available at http://rsb.info.nih.gov/ij; developed by Wayne Rasband, National Institutes of Health, Bethesda, MD). The Just another colocalization plug-in (JaCoP) was used to calculate colocalization statistics (Bolte and Cordelieres, 2006). Either deconvolved optical sections, or confocal sections were used for the colocalization analysis. Confocal microscopy was the preferred method of image acquisition for colocalization analysis. Colocalization analysis on deconvolved images required z-stacks to be deconvolved with a modification of the constrained iterative algorithm and display mapping set to clip. Images processed in this manner are a true representation of the original image and are reliable for quantitative microscopy. However, deconvolution using the constrained iterative algorithm is computationally intensive and can require up to 10 hours of processing time per z- stack. For large data sets deconvolution microscopy becomes impractical. For colocalization analysis merged, two color confocal or deconvolved sections were opened in imageJ and a region of interest was manually drawn around each cell. The area outside of the region of interest was cleared and set to pixel intensity value of zero. Merged color images were then separated into individual red, green, and blue components using the RGB split feature. Thresholds were set above background for each channel using the imageJ software and Manders M1 and M2 coefficients, Pearsons correlation coefficients, and overlap coefficients k1, and k2 were calculated using the JaCoP plug-in.

Manders coefficients M1 and M2 provide a more sensitive measure of channel1/channel2 overlap, and channel2/channel1 overlap respectively, and are not sensitive to variations in image intensity. Additionally, Manders coefficients can be directly interpreted as percent overlap, and thus were chosen as the preferred colocalization statistic for our experiments. To validate the colocalization procedure, we set up a series of test slides designed to demonstrate minimum and maximum colocalization. For maximal colocalization FITC labeled anti-ErbB2 (clone N28) was internalized into GA treated cells for 1 hour, followed by acid stripping, processing for IF, and then detection with a Texas Red labeled Goat anti-mouse secondary antibody. To test for minimum colocalization, Alexa-594 transferrin was internalized into cells for 5 minutes. The cells were then acid stripped, processed for IF, and stained with Anti-GM130 and DATF goat anti-mouse to label the trans-golgi network. Confocal sections were obtained and the colocalization procedure performed on these sections. We found that M1 and M2 values ranged from 0.7-.85 for the maximal colocalization slides and 0.05.-0.20 for minimal colocalization slides (See Figure 17).

Cell-based ELISA (CELISA) to Measure ErbB2 or Tf Internalization

SKBr3 cells seeded in 35 mm dishes the day before the assay (3 x 10^5 cells/dish) were pretreated with GA and other drugs as appropriate for 45 minutes. To measure ErbB2 internalization, biotinylated anti-ErbB2 antibodies (15 μg/ml)

were bound for 2 hours at 4°C. After washing with Hanks' balanced salt solution (GIBCO, Invitrogen), prewarmed media was added for various times to allow internalization. Internalization was stopped by washing with ice-cold Hanks' balanced salt solution and transferring dishes to ice. To mask residual surface-bound antibodies, cells were incubated with streptavidin (40 μg/ml) for 1 hour at 4°C. After washing, cells were paraformaldehyde-fixed, permeabilized, and blocked as for IF. Cells were then incubated with peroxidase-conjugated streptavidin polymer (1 μg/ml in PBS with 0.05% Tween 20) for 1 hour at room temperature. After washing, SureBlue Reserve tetramethylbenzidine (TMB) substrate (KPL, Gaithersburg, MD) was added for 10 sec, before stopping the reaction with TMB stop solution and measuring absorbance (450 nm) in a spectrophotometer. Background (signal in control dishes left on ice) was subtracted from all values. The same method was used to measure Tf uptake, except that biotinylated anti-ErbB2 antibodies were omitted, and biotinylated Tf (75 μg/ml) was not pre-bound, but added to media for the indicated times of uptake. Addition of 10-fold excess unlabeled Tf during a 20 minute uptake reduced the signal to background levels (A. G. Ostermeyer-Fay, unpublished).

Other Methods

For Fig. 12, sodium dodecyl sulfate polyacrylamide gel electrophoresis (SDS-PAGE), transfer to polyvinylidene difluoride, Western blotting, and detection by enhanced chemiluminescence were performed as described (Arreaza *et al.*, 1994). Bands were scanned and quantitated using NIH Image. For Fig. 13G,H, after transfer to nitrocellulose and incubation with appropriate primary antibodies, bands were labeled with AF680-secondary antibodies and detected and quantitated with the Odyssey-Infrared Imaging System (LI-COR Biosciences, Lincoln, NE), using the Odyssey imaging software.

Chapter 3. Clathrin-Independent Endocytosis of ErbB2 in Geldanamycin-Treated Human Breast Cancer Cells

Introduction

In this chapter we examined the internalization of ErbB2 in GA treated SKBr3 human breast cancer cells. An earlier study found that ErbB2 was internalized by the clathrin mediated pathway (Austin *et al.*, 2005). In contrast, we found that ErbB2 is internalized by a clathrin-independent pathway. ErbB2 Internalization was not affected by clathrin inhibitors and did not require dynamin. In the context of known endocytic pathways ErbB2 internalization most closely resembled the GEEC pathway described earlier. ErbB2 was internalized together with GPI-anchored proteins, cholera toxin, and fluid into structures that resembled GEECs. After internalization ErbB2 was transported to early endosomes where it merged with clathrin cargos. It was then directed to through late endosomes to lysosomes for degradation.

Results

ErbB2 Internalization in GA-Treated SkBr3 Cells is Independent of Clathrin

ErbB2 was expressed at high levels on the surface of SKBr3 cells (Figure 1A), as reported previously (Austin *et al.*, 2004; Hommelgaard *et al.*, 2004). Also as reported (Austin *et al.*, 2004; Hommelgaard *et al.*, 2004), fluorescein-conjugated surface-bound anti-ErbB2 antibodies (Fl-anti-ErbB2) did not greatly affect ErbB2 localization after 2-3 hours of warming (Figure 1B). By contrast, after 2-3 hours GA treatment, anti-ErbB2 staining of intracellular puncta was very bright, while residual surface staining was greatly reduced (Figure 1C). As previously reported (Austin *et al.*, 2004; Hommelgaard *et al.*, 2004), internalized ErbB2 was first easily visible 30-45 minutes after GA treatment.

To determine whether ErbB2 was internalized by clathrin-mediated endocytosis in GA-treated cells, we first used chlorpromazine (CPZ), a cationic amphiphile that inhibits this pathway (Wang *et al.*, 1993). CPZ efficiently inhibited uptake of AF-594 Tf, but did not block ErbB2 internalization (Figure 1D,E). After CPZ treatment, structures containing internalized ErbB2 sometimes had a tubular morphology (Figure 2A). This effect may have resulted from the ability of CPZ to induce membrane curvature (Lange and Steck, 1984). After longer, 30 minute internalizations in CPZ treated cells Tf and ErbB2 were both internalized and localized to enlarged endosomes (Figure 2B). This probably resulted because CPZ dramatically slows Tf internalization but it is not

completely blocked. CPZ treatment may in turn interfere with recycling resulting in Tf becoming trapped in enlarged endosomes after long periods of internalization. We quantitated the effect of CPZ on initial internalization of ErbB2 and Tf using a CELISA assay. CPZ inhibited uptake of biotinylated Tf in GA-treated SKBr3 cells (Figure 1F), but did not affect the internalization of surface-bound biotinylated anti-ErbB2 antibodies (Figure 1G).

We next determined whether ErbB2 colocalized with markers of the clathrin pathway very soon after internalization in GA-treated cells. ErbB2 did not co-localize significantly with clathrin (Figure 3). We saw some colocalization of ErbB2 with co-internalized rhodamine-conjugated Tf (Rh-Tf), to a degree that varied between cells. Nevertheless, most ErbB2-positive puncta did not label for Rh-Tf (Figures 1,4). By contrast, EGFR colocalized to a greater degree with clathrin (Figure 3), and EGFR and Rh-Tf co-localized substantially with each other (Figure 4). ErbB2-positive structures often had a distinctive morphology, captured most clearly in favorable epifluorescence images (Figure 4, row B): either short tubules, or round structures that were larger than the earliest, most peripheral Tf-containing vesicles, and had visible lumens. This image also showed that ErbB2-positive structures remained closer to the plasma membrane than Rh-Tf-positive structures after 5 minutes of internalization. These results showed that ErbB2 did not colocalize with markers of the clathrin-dependent

internalization pathway soon after internalization in GA-treated cells, and suggested that it was internalized by a different mechanism.

Eps15 associates with components of the clathrin coat, and is required for clathrin-mediated uptake (Conner and Schmid, 2003). Dynamin proteins mediate endocytic vesicle scission and are required for both clathrin-mediated and caveolar endocytosis (Conner and Schmid, 2003). Dominant-negative (DN) forms of Eps15 and dynamin-1 had similar effects in GA-treated SKBr3 cells: Rh-Tf uptake was inhibited, while ErbB2 internalization was still detected (Figure 5). That is, transient expression of DN-Eps15 (Figure 5A) or DN-dynamin (Figure 5B) inhibited Tf internalization compared to that in untransfected cells on the same slide, but did not block ErbB2 internalization. Results were quantitated (Figure 5C,D) by scoring transfected and untransfected cells either positive (at least 3 stained intracellular puncta) or negative for internalization of ErbB2 and Tf.

Together, these results showed that ErbB2 was internalized primarily by a clathrin-independent mechanism in GA-treated SKBr3 cells. Our next goal was to characterize ErbB2 internalization further in comparison to other clathrin-independent endocytic pathways.

ErbB2 Internalization Does Not Require Tyrosine Kinase Activity

As SKBr3 cells do not express caveolin-1 and lack caveolae (Hommelgaard *et al.*, 2004), ErbB2 cannot be internalized by caveolar endocytosis in these cells. However, a "caveolar-like" pathway, followed by cargoes normally internalized in caveolae, has been reported in some cells that lack caveolae. Endocytosis by this pathway is inhibited by the broad-specificity tyrosine kinase inhibitor genistein (Sharma *et al.*, 2004; Damm *et al.*, 2005). To see whether ErbB2 followed this pathway, we next determined whether ErbB2 internalization was sensitive to genistein. As a positive control for the efficacy of the drug, we verified that genistein inhibited EGF-induced stimulation of tyrosine kinase activity and internalization of tyrosine-phosphorylated substrates. SKBr3 cells express EGFR, though at much lower levels than ErbB2 (Beerli *et al.*, 1995). In untreated serum-starved cells and in cells treated with GA alone (Figure 6A, middle), anti-phosphotyrosine staining was largely restricted to the plasma membrane. Phosphotyrosine staining was dim in most cells, and was localized to the plasma membrane even in occasional brighter cells. However, after EGF treatment, internal puncta stained brightly with anti-phosphotyrosine antibodies (Figure 6B, middle). As reported earlier (Wang *et al.*, 1999; Haslekas *et al.*, 2005), EGF treatment did not significantly alter the distribution of ErbB2 in these cells (Figure 6B, top). As expected, both ErbB2 and tyrosine-phosphorylated substrates were internalized in cells treated with EGF and GA together (Figure

6C). Genistein essentially blocked tyrosine phosphorylation in cells treated with EGF and GA, but ErbB2 internalization remained robust (Figure 6D). We quantitated the effect of genistein on ErbB2 internalization by CELISA. Genistein did not inhibit, and in fact slightly stimulated, ErbB2 internalization (Figure 6E). This result is consistent with a previous report that ErbB2 internalization in GA-treated cells does not require its tyrosine kinase activity (Xu *et al.*, 2001), and suggests in addition that no other tyrosine kinase is required.

ErbB2 Colocalizes With AF-594-CTxB, PLAP, and a Fluid Phase Marker After a Short Time of Internalization

Mayor and colleagues reported that glycosyl phosphatidylinositol (GPI)-anchored proteins are constitutively taken up by a clathrin- and caveolin-independent mechanism into GPI-anchored protein-enriched early endosomal compartments (GEECs), which contain significant amounts of internalized fluid (Sabharanjak *et al.*, 2002; Kalia *et al.*, 2006). CTxB binds the ganglioside GM1 and is internalized by a variety of pathways, including clathrin-mediated and caveolar endocytosis (Lencer and Saslowsky, 2005). In at least some cell types, most CTxB is co-internalized with GPI-anchored proteins into structures with ring-shaped or tubular morphology termed clathrin-independent carriers (CLICs) (Kirkham *et al.*, 2005). The presence of GPI-anchored proteins in CLICs suggests that they may be the same as GEECs. After 5 minutes of uptake in GA-

treated SKBr3 cells, internalized ErbB2 colocalized extensively with co-internalized AF-594-CTxB, GPI-anchored PLAP, and the fluid phase marker dextran (Figure 7). A maximum-intensity projection image of a cell stained for co-internalized ErbB2 and CTxB is shown in Figure 7A. An enlarged section of the same cell (indicated by asterisks in Figure 7A) is shown in Figure 7B, in which both separate red and green channels (left and middle panels) and a merged image (right panel) are shown. Figure 7C,D display the edges of individual cells, at the same magnification as in Figure 5B, showing good colocalization of ErbB2 and PLAP (Figure 7C) or ErbB2 and dextran (Figure 7D) after 5 minutes of internalization. These observations suggest that ErbB2 is initially taken up by a pathway similar to those described earlier (Sabharanjak *et al.*, 2002; Kirkham *et al.*, 2005; Kalia *et al.*, 2006). When we quantified the amount of colocalization we found that after 2 minutes PLAP and CTxB colocalized significantly with ErbB2, whereas Tf did not (Figure 8).

ErbB2 is Transported to Early and Late Endosomes and is Degraded in Lysosomes in GA-treated Cells

We next examined downstream trafficking of ErbB2 in GA-treated cells. Although ErbB2 showed little co-localization with markers of the clathrin pathway after short internalization times in GA-treated cells (Figure 3,4,8), it colocalized significantly with Rh-Tf after longer times (Figure 9,10A). This

suggested that the ErbB2 transport pathway merged with the classical endocytic pathway following internalization. Consistent with this idea, and in agreement with an earlier report (Austin *et al.*, 2004), after 2 hours GA treatment, ErbB2 colocalized with the early endosome markers EEA1 and Rab5 (Figure 10B,C), and, as shown in Figure 10D, accumulated inside enlarged endosomes present in cells expressing constitutively active Rab5Q79L (Stenmark *et al.*, 1994). ErbB2 was sometimes detected inside structures surrounded with EEA1 in an irregular form (Figure 10B). These structures are probably the same as immature CD63-negative MVBs, surrounded by Tf-positive tubules, in which ErbB2 was detected in the interior vesicles by electron microscopy after 3 hours GA treatment (Austin *et al.*, 2004). The irregular appearance of EEA1 may reflect its localization in these tubules. After prolonged GA treatment, ErbB2 also colocalized with the late endosomal markers GFP-Rab7 and CD63 (Figure 11). Austin et al. reported little colocalization of ErbB2 with late endosome markers after 3 hours GA treatment (Austin *et al.*, 2004). This might have resulted from rapid degradation following delivery to lysosomes. Consistent with this possibility, as shown in Figure 11C and E, ErbB2 colocalized extensively with CD63 and LAMP1 after treating cells with GA together with chloroquine (CQ), which causes acidic compartments to swell and inhibits lysosomal degradation but not endocytic transport (Vonderheit and Helenius, 2005). Together, these results suggested that after internalization by a clathrin-independent pathway, ErbB2 is rapidly

transported to early and then late endosomes and finally to lysosomes for degradation.

To test this possibility further, we examined ErbB2 degradation in GA-treated SKBr3 cells by Western blotting. Consistent with an earlier report (Tikhomirov and Carpenter, 2000), a fragment of about 135 kDa that reacted with extracellular domain-specific anti-ErbB2 antibodies accumulated in lysates of cells treated with GA and CQ (Figure 12A, arrow). Full-length ErbB2 also appeared to be stabilized under these conditions. Including both full-length and 135 kDa forms of the protein in the quantitation, we found that CQ significantly slowed ErbB2 degradation (Figure 12B). Thus, consistent with earlier results (Tikhomirov and Carpenter, 2000; Lerdrup *et al.*, 2006), at least a major fraction of ErbB2 is degraded in lysosomes.

ErbB2 Accumulates in Vesicles Containing Constitutively-Active Arf6-Q67L Only in the Absence of GA

Donaldson and colleagues have described a non-clathrin-mediated endocytic pathway that is regulated by Arf6 (Naslavsky *et al.*, 2003, , 2004). Expression of constitutively-active Arf6Q67L causes cargo of this pathway accumulate in Arf6Q67L-positive endosomes, which are often enlarged. To determine whether ErbB2 followed this pathway, we expressed HA-tagged Arf6-Q67L in SKBr3 cells, treated cells with GA, and examined the localization of

Arf6-Q67L and ErbB2. Although Arf6-Q67L-positive endosomes were seen, ErbB2 did not accumulate in them (Figure 13A). Instead, ErbB2 showed partial colocalization with GFP-Rab5 and GFP-Rab7, showing that it reached early and late endosomes even in the presence of Arf6-Q67L (Figure 13B,C). Furthermore, Arf6Q67L did not affect ErbB2 degradation in GA-treated COS cells co-transfected with ErbB2 and Arf6Q-67L (Figure 13G,H). (Western blotting showed that transfected ErbB2 was at least 5-10 times more abundant than endogenous ErbB2 in COS-7 cells, and imunofluorescence analysis showed that at least 80% of transfected cells that expressed ErbB2 also expressed Arf6-Q67L.) By contrast, ErbB2 accumulated in Arf6-Q67L-positive endosomes, rather than Rab5- or Rab7-positive endosomes, when cells were not treated with GA (Figure 13D-F). Thus, ErbB2 followed the Arf6-regulated pathway in untreated cells. GA altered the internalization or downstream trafficking of ErbB2, preventing it from accumulating in Arf6-Q67L-positive endosomes.

DISCUSSION

ErbB2 is Internalized by a Clathrin-Independent Pathway

We found that ErbB2 is internalized by a clathrin-independent pathway in GA-treated SKBr3 cells. By contrast, Austin et al. reported that several inhibitors of the clathrin pathway inhibited ErbB2 uptake under the same conditions (Austin *et al.*, 2005). We do not know the explanation for this difference. Austin et al. assayed for inhibition of internalization by binding labeled anti-ErbB2 antibodies to cells, warming for 3 hours with or without inhibitors, and then measuring the amount of internalized antibodies. It is possible that the effects observed after this prolonged internalization time resulted from inhibition of recycling, rather than of initial internalization. In fact, we noticed that prolonged CPZ treatment caused Tf as well as ErbB2 to accumulate in enlarged endosomes, suggesting that recycling was inhibited (Figure 2).

Why EGFR but not ErbB2 is Targeted to Clathrin-coated Pits

EGFR is one of the best-studied cargoes of the clathrin pathway. Because EGFR and ErbB2 are very similar, it may seem surprising that ErbB2 is not targeted to this pathway. However, recent findings on trafficking of EGFR and other ErbB family members can help explain this finding.

EGFR internalization does not depend on the clathrin adaptor AP2 (Hinrichsen *et al.*, 2003; Motley *et al.*, 2003). Instead, EGFR internalization

requires Grb2 (Wang and Moran, 1996; Jiang *et al.*, 2003) and c-Cbl or the related protein cbl-b (Ettenberg *et al.*, 1999; Levkowitz *et al.*, 1999). c-Cbl binds tyrosine-phosphorylated EGFR both directly, through its SH2 domain (Galisteo *et al.*, 1995; Levkowitz *et al.*, 1999), and indirectly, via Grb2 (Meisner and Czech, 1995; Fukazawa *et al.*, 1996; Jiang *et al.*, 2003), and ubiquitinates EGFR.

c-Cbl binds only to tyrosine-phosphorylated EGFR. By contrast, internalization of ErbB2 in GA-treated cells does not require tyrosine phosphorylation. Furthermore, ErbB family members other than EGFR do not recruit c-Cbl even when activated (Levkowitz *et al.*, 1996; Muthuswamy *et al.*, 1999). Even activated EGFR-ErbB2 heterodimers fail to bind c-Cbl, probably because ErbB2 is unable to phosphorylate the c-Cbl binding site on EGFR (Muthuswamy *et al.*, 1999). This could explain reports that found that EGFR is the only ErbB family member that is rapidly down-regulated upon activation (Stern *et al.*, 1986; King *et al.*, 1988; Lenferink *et al.*, 1998), as well as chimeric receptor studies showing that the cytoplasmic domains of ErbB2-4 are internalization impaired (Sorkin *et al.*, 1993; Baulida *et al.*, 1996; Waterman *et al.*, 1999). As expected, heterodimerization with ErbB2 inhibits EGFR down-regulation following ligand binding (Lenferink *et al.*, 1998; Muthuswamy *et al.*, 1999; Wang *et al.*, 1999; Lidke and Arndt-Jovin, 2004; Haslekas *et al.*, 2005).

It is not clear how c-Cbl stimulates EGFR internalization. According to one model, ubiquitinated EGFR is recognized by ubiquitin-binding domains of

accessory proteins associated with the clathrin coat (Haglund *et al.*, 2003; de Melker *et al.*, 2004b; Stang *et al.*, 2004; Fallon *et al.*, 2006). Alternatively, ubiquitination may target EGFR for clathrin-independent internalization (Sigismund *et al.*, 2005). By contrast, other workers have proposed that ubiquitination is not required for EGFR internalization (Duan *et al.*, 2003), and that the essential role of c-Cbl in EGFR internalization is independent of ubiquitination (Soubeyran *et al.*, 2002; Jiang and Sorkin, 2003; Huang *et al.*, 2006). In fact, Lys-mutants of EGFR showing a 70-80% reduction in ligand-stimulated ubiquitination are internalized normally (Huang *et al.*, 2006). A ubiquitin-independent role of c-Cbl in EGFR internalization would likely involve a complex of c-Cbl, CIN85, and endophilin reported to be required for EGFR endocytosis (Soubeyran *et al.*, 2002). Though this controversy has not yet been resolved, an essential role for c-Cbl in efficient EGFR internalization seems clear. The failure of ErbB2 to bind c-Cbl could explain why it is not targeted to clathrin-coated pits.

If ubiquitination does signal EGFR internalization, then ubiquitination of ErbB2 by CHIP could be imagined to play a similar role - possibly targeting ErbB2 for clathrin-independent internalization, as reported for EGFR (Sigismund *et al.*, 2005). Further work will be required to fully characterize the role of ubiquitination in ErbB2 trafficking.

Relation of ErbB2 Endocytosis to Other Non-Clathrin Pathways

ErbB2 internalization in SKBr3 cells did not occur via caveolae, as these cells lack caveolae (Hommelgaard *et al.*, 2004). Furthermore, unlike caveolar endocytosis (Henley *et al.*, 1998) and also unlike a pathway used to internalize the interleukin-2 receptor in lymphocytes (Lamaze *et al.*, 2001), ErbB2 internalization did not require dynamin function. ErB2 internalization differed from a "caveolar-like" pathway that operates in cells lacking caveolae (Damm *et al.*, 2005) in not requiring tyrosine kinase activity.

ErbB2 internalization was similar to GEEC and CLIC pathways (Sabharanjak *et al.*, 2002; Kirkham *et al.*, 2005; Kalia *et al.*, 2006) and to the Arf6-regulated pathway. That is, uptake did not require clathrin, dynamin, or caveolae. In addition, internalized ErbB2 colocalized with a GPI-anchored protein, CTxB, and a fluid phase marker. Structures containing newly-internalized ErbB2 often had the distinctive appearance of CLICs. Furthermore, following internalization, ErbB2 was delivered to early endosomes that also contained clathrin-dependent cargo.

ErbB2 accumulated in Arf6-Q67L-positive endosomes in control cells, showing that it followed the Arf6-regulated pathway. However, ErbB2 did not accumulate in these structures after GA treatment. It is possible that ErbB2 is internalized by different pathways with and without GA treatment, and that GA causes ErbB2 to by-pass the Arf6-regulated compartment. An alternate

explanation, which we favor, is that ErbB2 is internalized by the same pathway under both conditions, but avoids entrapment in the Arf6-Q67L endosomes in the presence of GA. The idea that ErbB2 may be internalized both with and without GA treatment is consistent with results of Austin et al. (Austin *et al.*, 2004). In contrast to another group (Hommelgaard *et al.*, 2004), these authors found that ErbB2 is internalized constitutively, but normally recycles efficiently to the plasma membrane. They proposed that GA affects ErbB2 trafficking only in endosomes, diverting the protein from the recycling pathway into MVBs (Austin *et al.*, 2004). In the context of this model, Arf6Q67L may prevent ErbB2 from recycling, causing it to accumulate in swollen vacuoles in the absence of GA. By contrast, Arf6-Q67L may not inhibit ubiquitin-based sorting into MVBs and downstream transport lysosomes. Our finding contrasts with an earlier report that Arf6-Q67L inhibited transport of MHC Class I protein and CD59 to lysosomes for degradation (Naslavsky *et al.*, 2004), possibly reflecting the fact that ErbB2 is ubiquitinated.

How ErbB2 Might be Targeted for Internalization

We do not know what targets ErbB2 for internalization by the pathway we have described. A clue may come from the characteristics of the GEEC/CLIC pathway(s) (Sabharanjak *et al.*, 2002; Kirkham *et al.*, 2005; Kalia *et al.*, 2006). Both GPI-anchored proteins and CTxB have a high affinity for lipid rafts, or

membrane microdomains in the liquid-ordered phase. ErbB2 can be enriched in detergent-resistant membranes, an indication of high raft affinity (Zhou and Carpenter, 2001; Nagy *et al.*, 2002; Hommelgaard *et al.*, 2004; Yang *et al.*, 2004; Zurita *et al.*, 2004). Thus, a subset of transmembrane proteins with high raft affinity may be targeted to the GEEC/CLIC pathway. Alternatively, ErbB2 may internalized by a bulk membrane pathway, without recognition of specific signals. This might explain why such a wide variety of proteins is internalized by this pathway in unstimulated cells.

Downstream Trafficking of ErbB2

As reported previously (Austin *et al.*, 2004), ErbB2 was transported to EEA1-positive early endosomes after internalization. The earlier workers also found ErbB2 in vesicles inside MVBs in GA-treated cells, suggesting transport to degradative compartments (Austin *et al.*, 2004). However, they noted that ErbB2-positive MVBs retained immature characteristics such as recycling tubules even after prolonged geldanamycin treatment. They were also surprised to see poor colocalization of ErbB2 with the late endosome marker CD63 (Austin *et al.*, 2004). By contrast, we saw good colocalization of ErbB2 with CD63 and LAMP1, especially after CQ treatment. We also found that ErbB2 degradation was inhibited by CQ when blots were probed with antibodies directed against the

extracellular domain of the protein, confirming previous work (Tikhomirov and Carpenter, 2000, , 2001) and suggesting that the apparent CQ insensitivity reported initially (Mimnaugh *et al.*, 1996; Citri *et al.*, 2002; Way *et al.*, 2004) resulted from inability of blotting antibodies to detect a clipped form of the protein. In summary, we showed that after GA treatment, ErbB2 is internalized by a non-clathrin, non-caveolar pathway, and then merges with the classical endocytic pathway for transport to lysosomes and degradation.

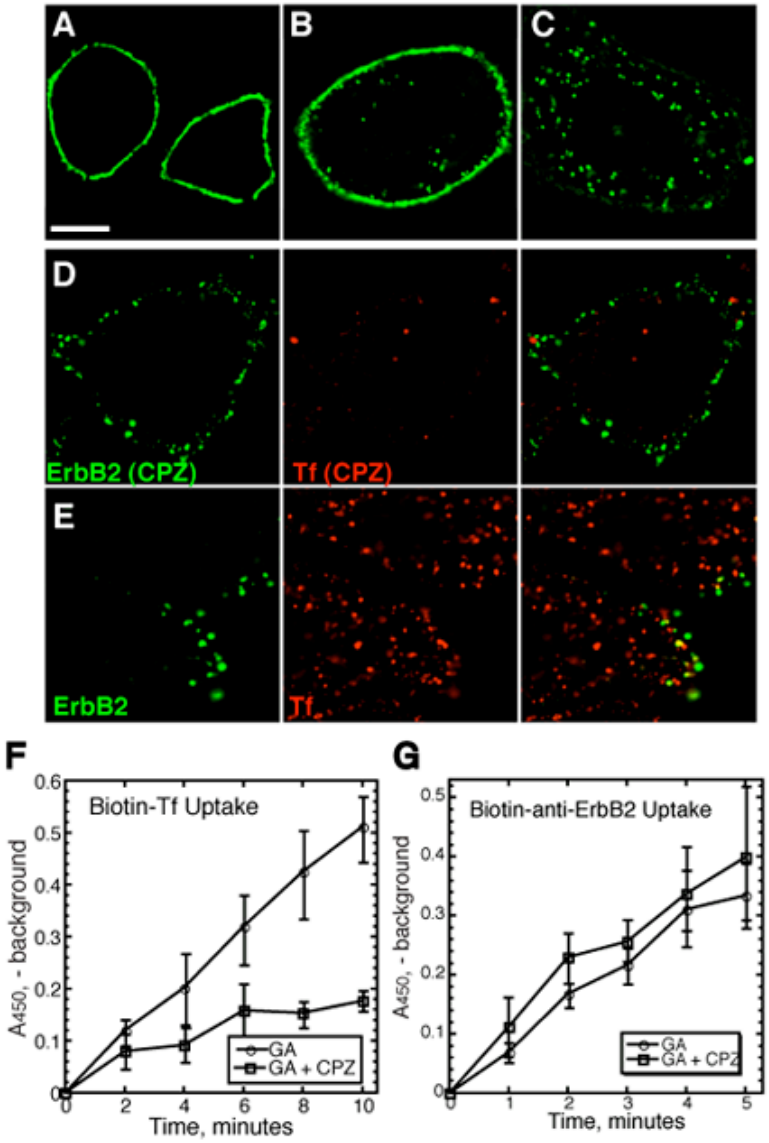

Figure 1. Effect of bound antibodies, GA, and CPZ on ErbB2 localization in SKBr3 cells. (A) ErbB2 was detected in fixed, permeabilized cells by indirect IF. (B) Cells were warmed for 2 hours after binding Fl-anti-ErbB2 before fixation. (C) Cells were treated with GA for 2 h before fixation, permeabilization, and detection of ErbB2 by indirect IF. (D,E) Cells were pre-treated for 45 minutes at 37°C with 5 μg/ml GA, with (D) or without (E) 12 μg/ml CPZ, before binding anti-ErBb2 antibodies and AF-594-Tf for 1 hour on ice and re-warming for 2 minutes with the same drugs. Cells were acid-washed and processed for immunofluorescence, detecting ErbB2 with the AF-488 Zenon mouse IgG labeling kit. (D,E) ErbB2, left; Tf, center; merged images, right. Scale bar (applies to all panels); 10 μm. (F,G) Internalization of biotinylated Tf (F) or biotinylated anti-ErbB2 antibodies (G) was measured by CELISA as described in Methods in cells treated with GA alone (circles) or both GA and CPZ (squares). A_{450} of each sample, after subtracting background, is shown. Values shown are the mean +/- s.e.m. of 3 experiments

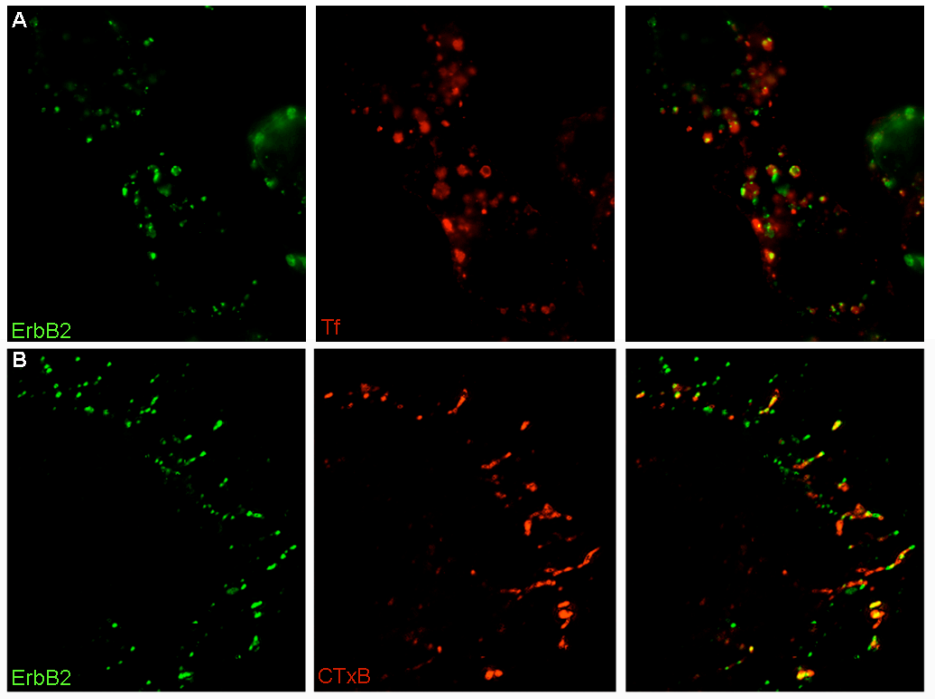

Figure 2. Effects of CPZ treatment. Cells were pretreated with 5 µg/ml GA and 8 µg/ml chlorpromazine, subjected to Fl-anti ErbB2 and Tf (A) or CTxB (B) binding and warmed for 30 (A) or 5 (B) minutes. Residual surface bound antibody was removed by acid stripping and the cells fixed. Figure A shows the enlarged endosomes containing Tf and ErbB2 that resulted after long warm-ups. B shows a representative example of the tubular morphology that occasionally results from CPZ treatment.

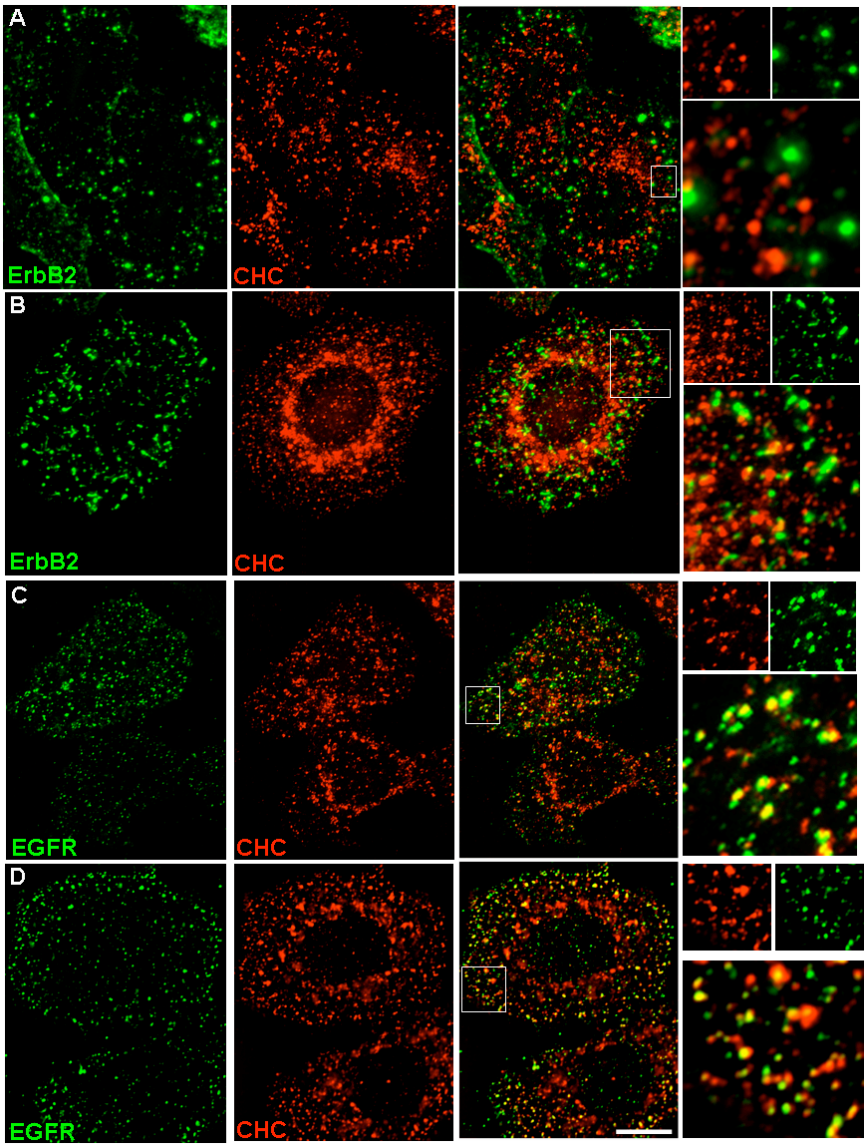

Figure 3. Localization of ErbB2, EGFR, and clathrin after 2 or 5 minutes internalization. SKBr3 cells were pre-treated with 5 μg/ml GA for 1 hour before binding Fl-anti-ErbB2 (A and B) or Fl-anti-EGFR (C and D) and warming for 2 minutes (A and C) or 5 minutes (B and D). Residual surface-bound antibody was removed by acid stripping, and the cells were fixed. Clathrin heavy chain (CHC) was detected by indirect IF using Texas red secondary antibodies. Green only panels are ErbB2 or EGFR as indicated, Red panels are clathrin heavy chain, and the merge of red and green channels are shown in the third column. A magnification of the boxed area in the merged images is shown in the far right hand column. All panels show maximum intensity projections of deconvolved Z-stacks. Scale bar; 10 μm.

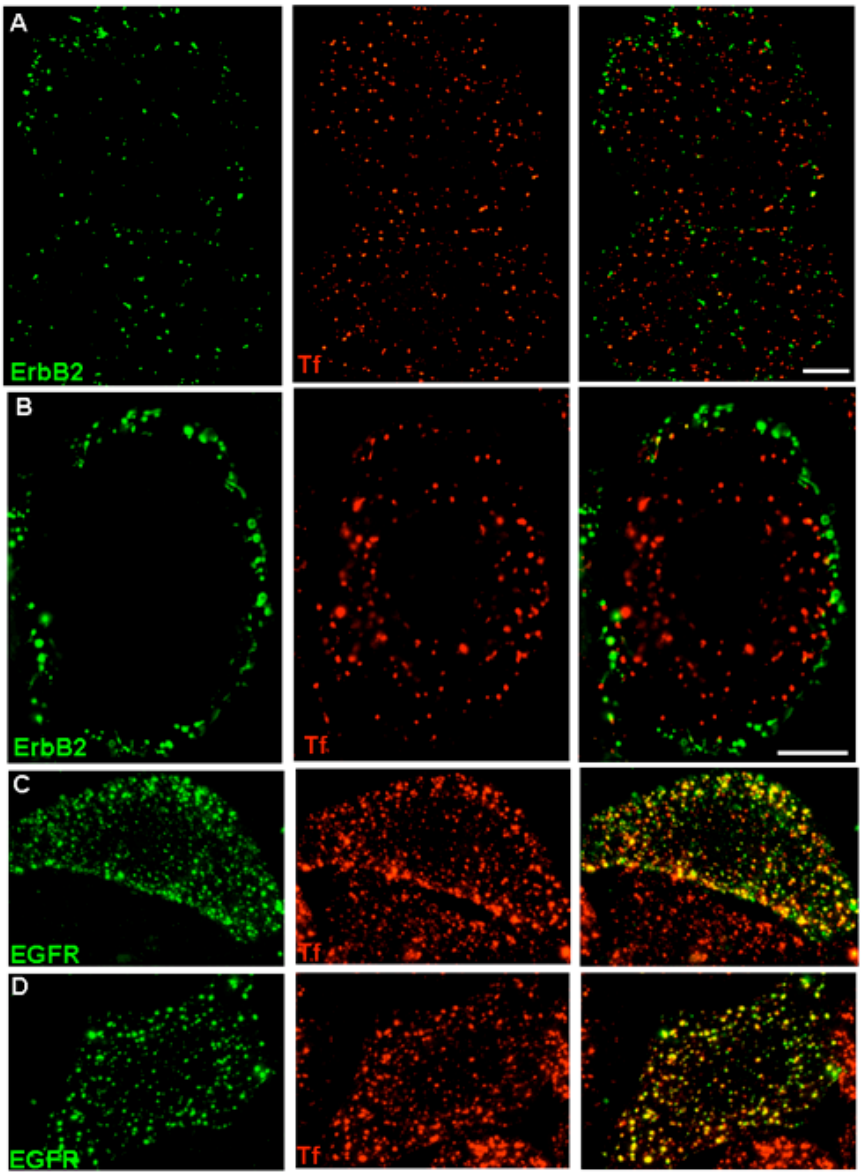

Figure 4. Localization of ErbB2, EGFR, and Transferrin (Tf) after 2 or 5 minutes internalization. SKBr3 cells were pre-treated with 5 μg/ml GA for 1 hour before binding 35 μg/ml Tf and Fl-anti-ErbB2 (A and B) or Fl-anti-EGFR (C and D) and warming for 2 minutes (A and C) or 5 minutes (B and D). Residual surface-bound antibody was removed by acid stripping, and the cells were fixed. Green panels are ErbB2 or EGFR as indicated, Red panels are Tf, and the merge of red and green channels are shown in the third column. Rows A, C, and D, show maximum intensity projections of deconvolved Z-stacks. Row b is an epifluorescence image. Scale bars; 10 μm.

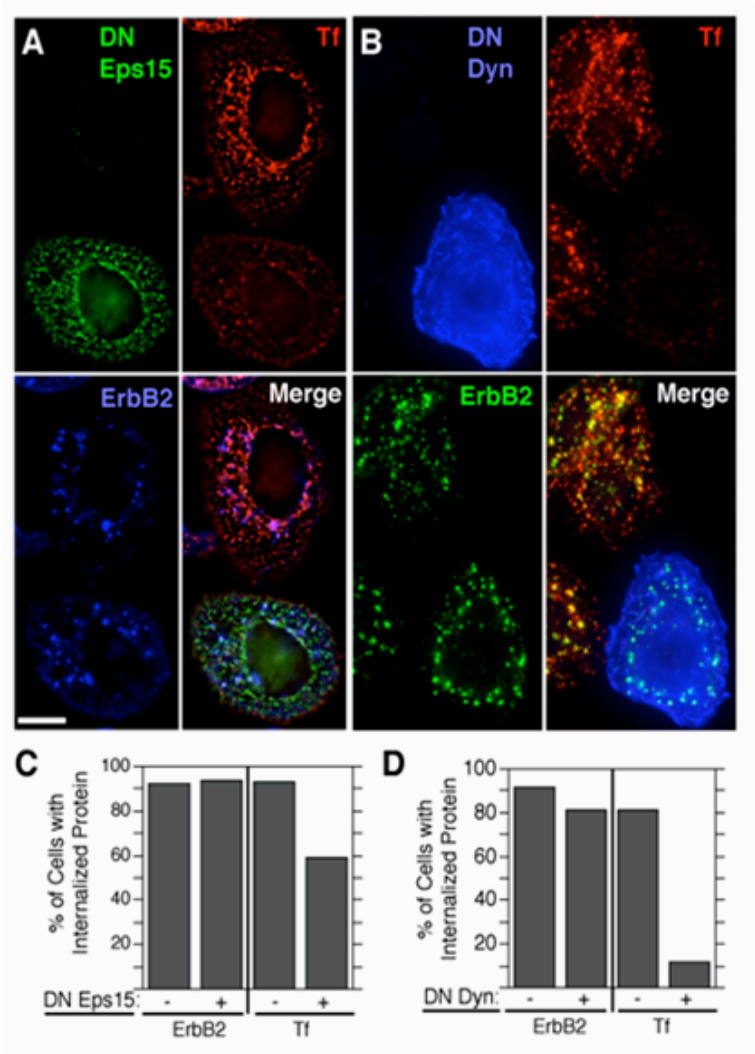

Figure 5. DN-Eps15 and DN-dynamin inhibit internalization of Rh-Tf but not ErbB2. SKBr3 cells transiently transfected with EGFP-DN-Eps15 (A,C) or HA-DN-dynamin-1 (B,D) were pretreated with GA for 2 hours before binding unlabeled anti-ErbB2 antibodies (A,C) or Fl-anti-ErbB2 antibodies (B,D), warmed for 30 minutes with Rh-Tf, fixed and permeabilized. (A,B) EGFP-DN-Eps15 (A, green) or DN-dynamin (B, blue, detected with anti-HA and AF-350 goat anti-rabbit IgG antibodies) are shown together with Rh-TF and ErbB2, as indicated, in deconvolved images, each from a Z-stack of a field in which one cell expressed DN-Eps15 (A) or DN-dynamin (B). ErbB2 was detected with AF-350 goat anti-mouse antibodies (A,C; blue) or by fluorescein fluorescence (B,D; green). Scale bar; 10 μm. (C,D) ErbB2 and Rh-Tf internalization were examined in cells expressing EGFP-DN-Eps15 (C) or DN-dynamin (D), and untransfected cells on the same coverslips. Cells showing at least three intracellular puncta were scored as positive for internalization. In each case, numbers shown are averages of two experiments (counting at least 100 transfected and 100 untransfected cells in each experiment) that varied by <10%.

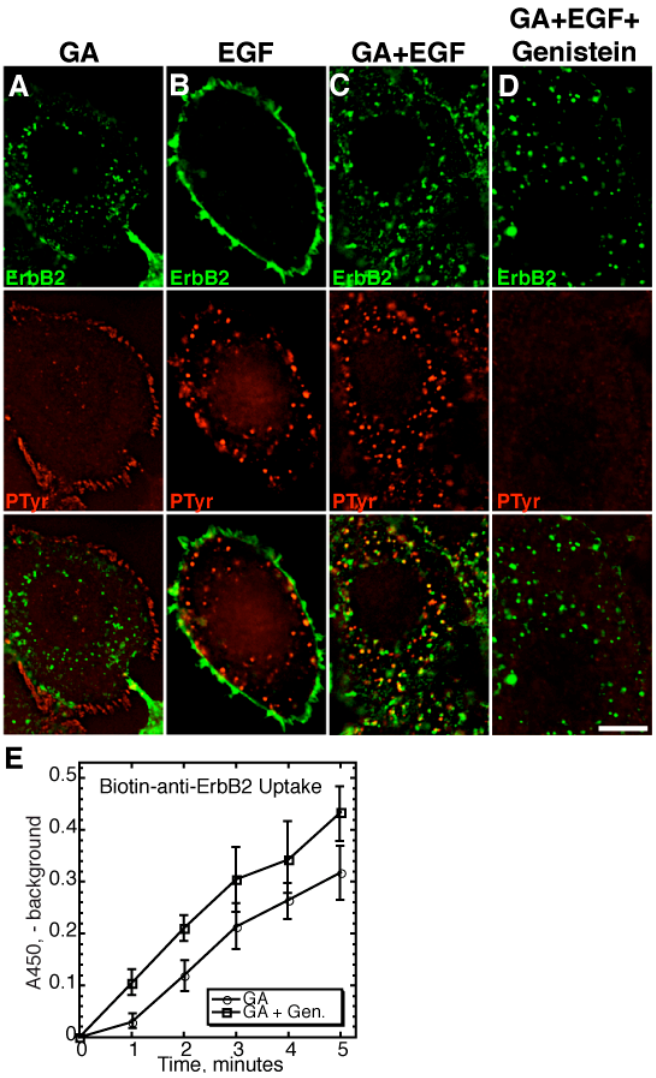

Figure 6. Genistein inhibits EGF-stimulated tyrosine kinase activity but not ErbB2 internalization. SKBr3 cells were serum-starved overnight, treated as described for individual panels, fixed, and permeabilized. Cells were treated with: (A) GA for 2 hours; (B) 100 ng/ml EGF for 10 minutes; (C) GA for 2 hours, with 100 ng/ml EGF added for the last 10 minutes; and (D) 100 μg/ml genistein for 1 hour, then with GA added for another 2 hours, with 100 ng/ml EGF added for the last 10 minutes. Deconvolved images from Z-stacks are shown. ErbB2 (green, top panels) was detected with polyclonal anti-ErbB2 antibodies and P-Tyr (red, middle panels) with monoclonal antibodies. Bottom panels; merged images. Scale bar; 10 μm. (E) SKBr3 cells were pre-treated with GA (circles) or GA + 100 μg/ml genistein (squares) for 45 minutes before binding biotinylated anti-ErbB2 antibodies and warming for 0-5 minutes in the presence of the same drugs. Internalized antibodies were quantitated by CELISA, as described in Methods. A_{450} of each background-subtracted sample is shown. Values shown are the mean +/- s.e.m. of 3 experiments.

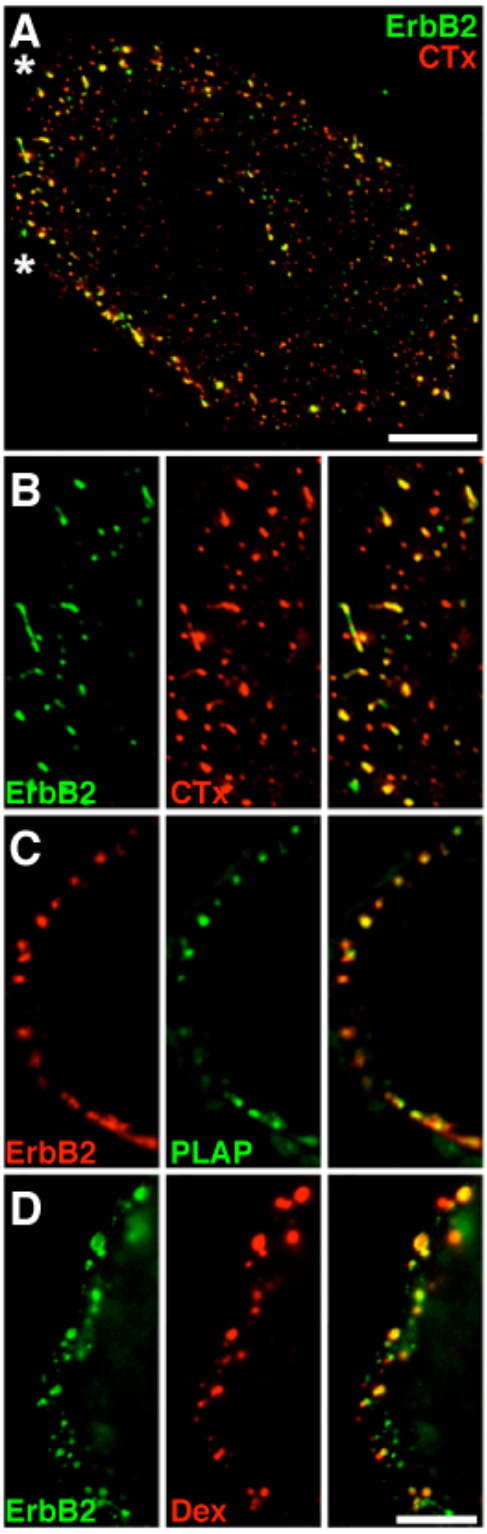

Figure 7. Co-localization of ErbB2 with AF-594-CTxB, PLAP, and dextran in SKBr3 cells after 5 minutes internalization. All cells were pre-treated with GA 1 hour, subjected to antibody or toxin binding on ice for 1 hour as appropriate, warmed for 5 minutes, acid-stripped, and fixed. (A) Fl-anti-ErbB2 and AF-594-CTxB (0.5 μg/ml) were bound to cells. A merged maximum intensity projection image of a deconvolved Z-stack is shown (ErbB2, green; AF-594-CTxB, red). Asterisks indicate region shown enlarged in B (ErbB2, left; AF-594-CTxB, middle; merged image, right). (C) Fl-anti-PLAP Fab fragments and Rh-anti-ErbB2 antibodies were bound to cells. A deconvolved image from a Z-stack, showing part of the edge of one cell, is shown. ErbB2, left; PLAP, middle; merged image, right. (D) Fl-anti-ErbB2 was bound to cells, which were warmed with 1 mg/ml FluoroRubyTM dextran. An epifluorescence image, showing part of the edge of one cell, is shown. ErbB2, left; dextran, middle; merged image, right. Scale bars; A, 10 μm; D (applies to B-D), 5

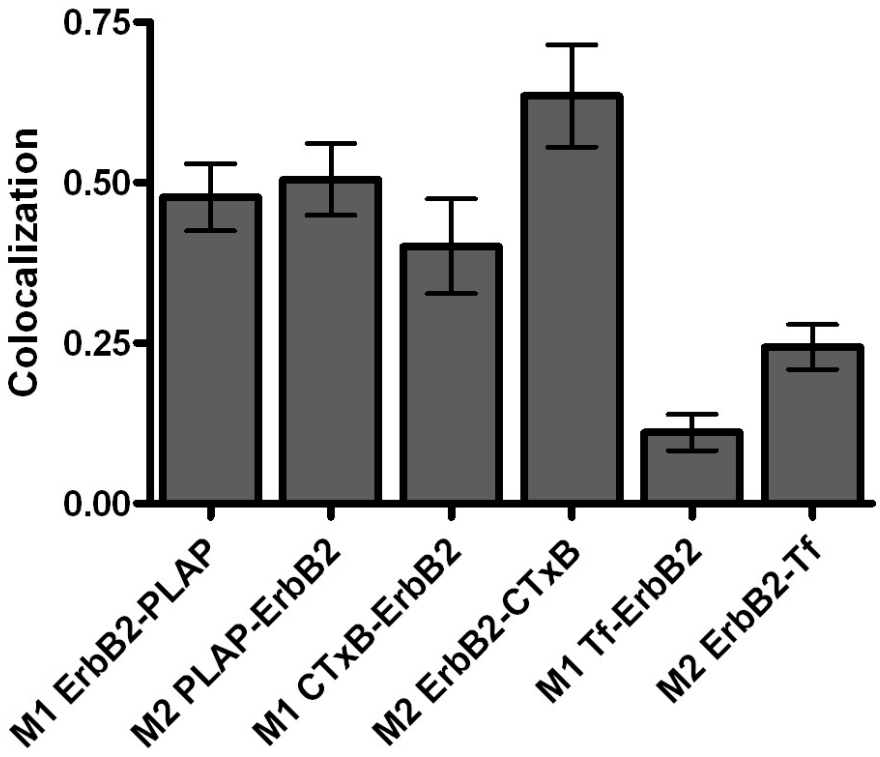

Figure 8. Quantitation of Co-localization of ErbB2 with AF-594-CTxB, PLAP, and Tf in SKBr3 cells after 2 minutes internalization. SKBr3 cells were pre-treated with GA for 1 hour, subjected to antibody, toxin and Tf binding for 1 hour and then warmed 2 minutes. Residual surface bound antibodies or toxin was removed by acid stripping and the cells were fixed. Images were acquired with a Zeiss laser scanning microscope. Airy units were set to 1 and levels for laser intensity and detector gain were optimized prior to image acquisition and kept constant for each slide. Bars represent the average of at least 10 cells. Error bars are standard error. Colocalization was performed as described in the methods and materials section.

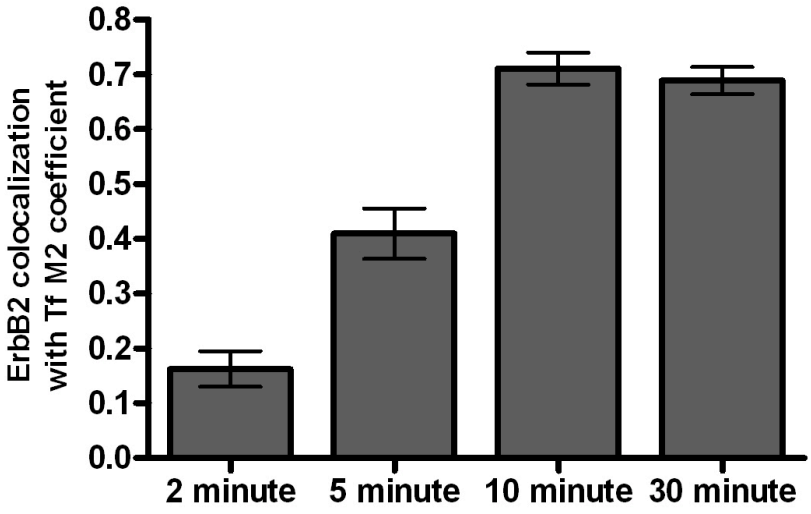

Figure 9. ErbB2 colocalization with Tf increases after 2 minutes. SKBr3 cells were treated with GA for 1 hour at 37 ºC. FITC- anti-ErbB2 antibodies and AF-594 Tf were bound in the cold, unbound antibody washed away and then warmed for 5-30 minutes. Z-stacks of individual cells were acquired and deconvolved by a modification of the constrained iterative algorithm. Colocalization analysis was performed on sections using the JACoP plug-in in imageJ. Manders coefficient M2 representing amount of ErbB2 overlapping Tf. Bars represent average of at least 10 cells. Error bars are SEM.

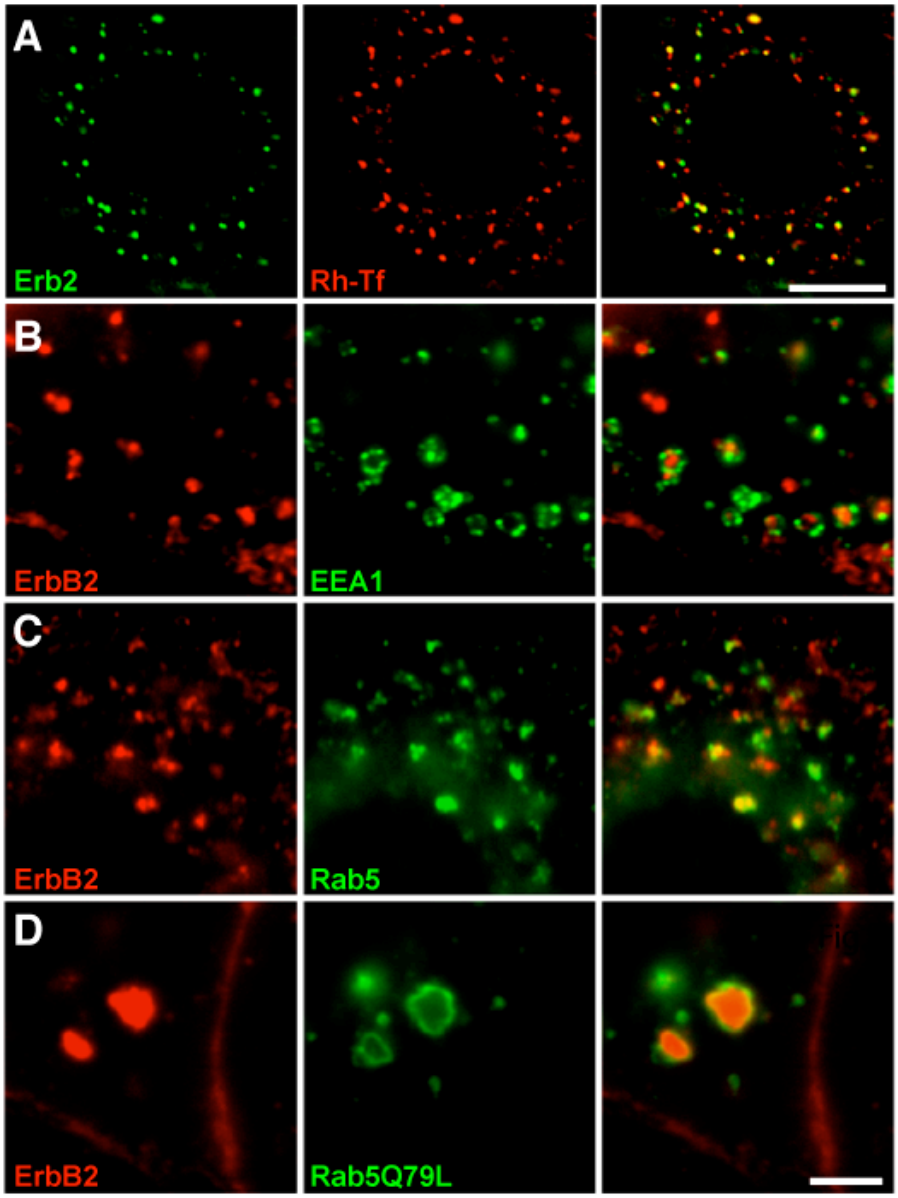

Figure 10. ErbB2 is delivered to early endosomes after GA treatment. SKBr3 cells were transiently transfected with GFP-Rab5 (C) or GFP-Rab5Q79L (D), treated with GA for 2 hours (in media containing Rh-Tf in A), fixed, and permeabilized. (A-D) Left panels; ErbB2, detected with polyclonal antibodies. Center panels: (A) Rh-Tf fluorescence; (B) endogenous EEA1; (C,D) GFP fluorescence. Right panels; merged images. (A) deconvolved image from a Z stack; (B-D) epifluorescence images. Scale bars; A, 10 μm; D (applies to B-D), 5 μm.

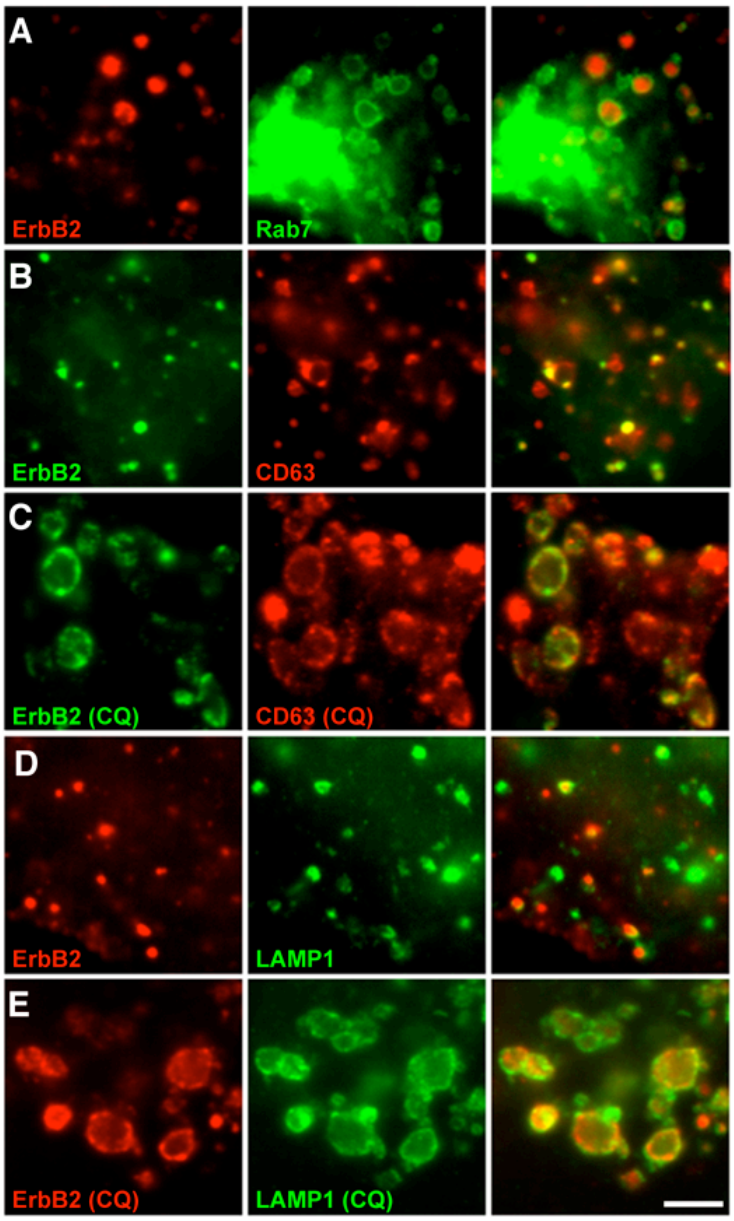

Figure 11. ErbB2 is delivered to late endosomes and lysosomes after GA treatment. After transient expression of GFP-Rab7 (A) SKBr3 cells were treated with GA for 5 hours, sometimes (C,E) together with 100 μM CQ, fixed, and permeabilized. Left panels; ErbB2 was detected with polyclonal (A-C) or monoclonal (D,E) antibodies and appropriate secondary antibodies. Middle panels: (A) Rab7 (GFP fluorescence); (B,C) endogenous CD63; (D,E) endogenous LAMP1. Right panels; merged images. Epifluorescence images are shown. Scale bar; 5 μm.

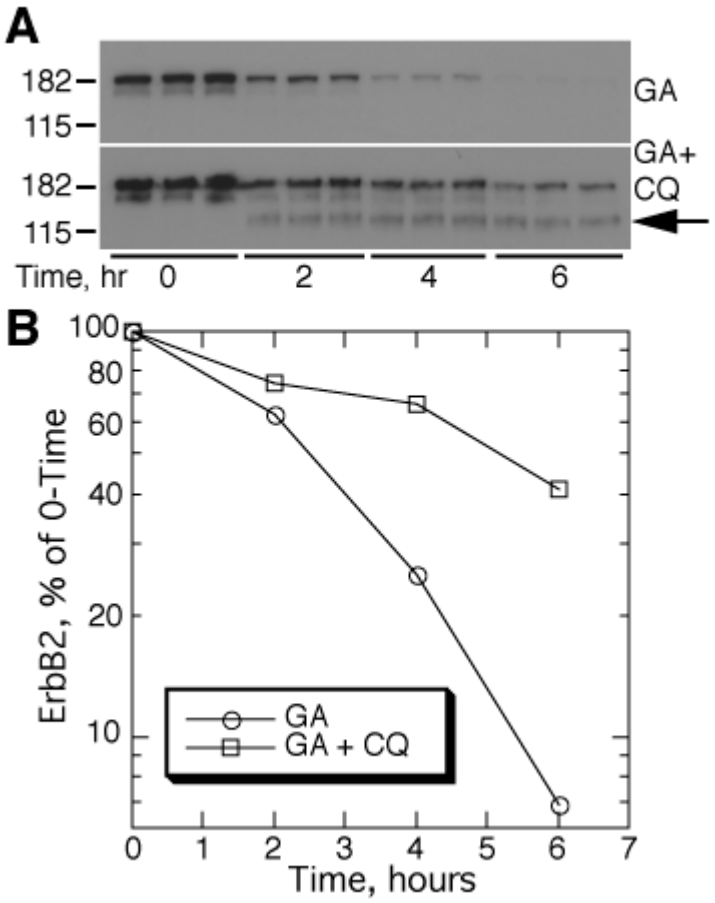

Figure 12. GA-induced ErbB2 degradation is sensitive to CQ. SKBr3 cells were incubated with GA with or without CQ for the times indicated and lysed. Proteins were separated by SDS-PAGE and transferred to membranes for Western blotting and detection of ErbB2. (A) Western blots. Top, GA alone; bottom, GA and CQ. Arrow; ca. 135 kDa ErbB2 fragment. (B) Bands were quantitated by scanning densitometry and plotted as % of 0-time signal remaining at each time.

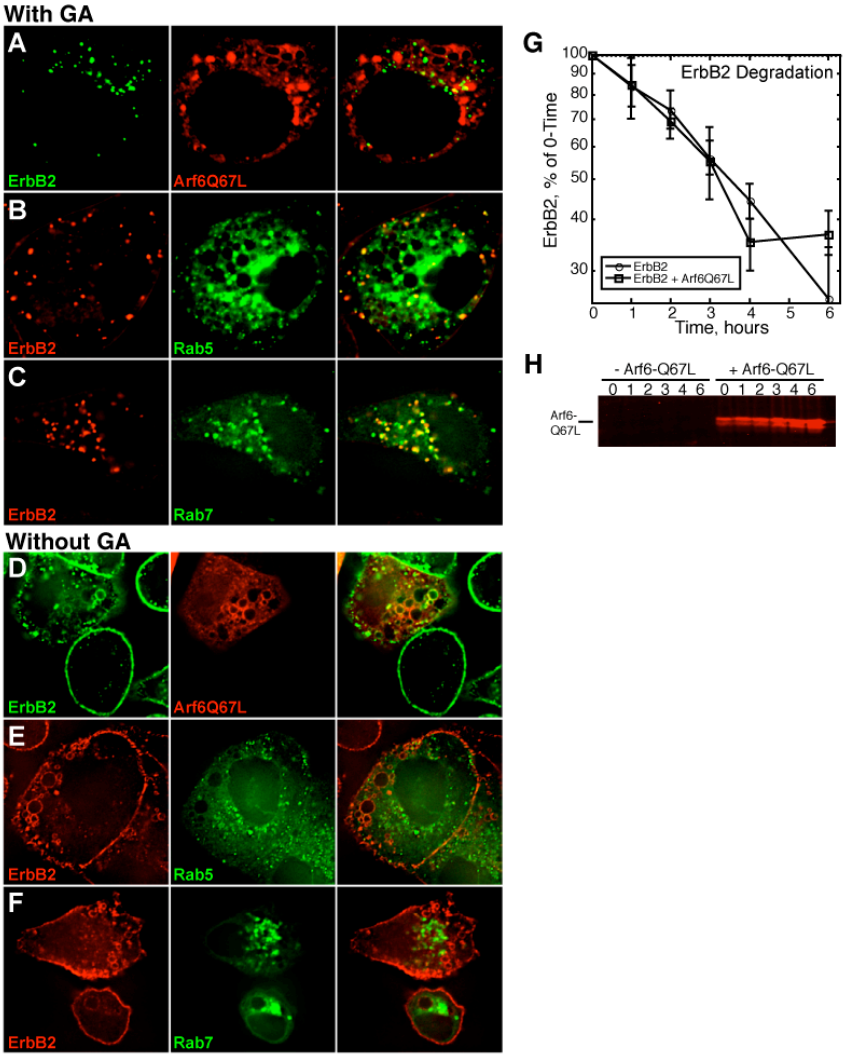

Figure 13. ErbB2 accumulates in Arf-Q67L-positive endosomes only in the absence of GA. (A-F) SKBr3 cells were transfected with Arf6-Q67L, either alone (A,D) or together with GFP-Rab5 (B,E) or GFP-Rab7 (C,F), and examined 14-16 hours after transfection. Fl-anti-ErbB2 (A,D) or unlabeled anti-ErbB2 antibodies (B,C,E,F) were bound for 1 hour at 4°C, and cells were then warmed for 2 hours with (A-C) or without (D-F) GA. Internalized anti-ErbB2 was detected in fixed and permeabilized cells by Fl-anti-ErbB2 fluorescence (A,D) or with Texas red goat-anti-mouse antibodies (B,C,E,F). Although Arf6Q67L was not visualized in B,C,E, or F, vacuoles characteristic of Arf6-Q67L expression were seen. (G,H) COS-7 cells were transfected with ErbB2 alone or together with Arf6-Q67L as indicated. Cells were incubated with GA for the indicated times and solubilized in gel loading buffer. Proteins were separated by SDS-PAGE and transferred to nitrocellulose. ErbB2 and Arf6-Q67L were detected by immunoblotting, using anti-ErbB2 antibody #20 and anti-HA antibodies respectively and AF680-secondary antibodies, and detecting and quantitating fluorescent bands using the Odyssey system. (H) A representative Arf6-Q67L blot is shown, demonstrating expression in co-transfected cells (+Arf6-Q67L), but not in cells expressing ErbB2 alone (-Arf6-Q67L).

Chapter 4. ErbB2 internalization through the GEEC pathway

Introduction

Data presented in the last chapter suggested that ErbB2 is internalized by the GEEC pathway in SKBR3 cells. That is, ErbB2 colocalized with the GPI-anchored protein PLAP, cholera toxin B subunit, and a fluid phase marker soon after internalization. Furthermore, newly-internalized ErbB2 was found in structures with a tubular or ring shaped morphology that resembled GEECs. The GEEC pathway was described as a constitutive endocytic pathway that is specific for GPI-anchored proteins, as transmembrane proteins were excluded from these structures in CHO cells (Sabharanjak *et al.*, 2002). Surprisingly, as detailed below, we found that chimeric fusion proteins of PLAP containing cytosolic and transmembrane domains also colocalized extensively with ErbB2 immediately after uptake in SKBr3 cells. It was possible that this effect was specific to SKBr3 cells. However, when ErbB2 was co-expressed with PLAP or the PLAP chimeras in CHO cells, we again saw strong colocalization. This was not specific to ErbB2 as the chimeric PLAP proteins also colocalized with the GPI-anchored protein Thy-1. Data in this chapter suggest that ErbB2 is internalized by the GEEC pathway in two cell types. However, our data suggest, in contrast to a previous report, that this pathway is not specific for GPI- anchored proteins. Together with

other results from our lab, these data suggest instead that the GEEC pathway probably represents a bulk internalization pathway that operates constitutively in multiple cell types.

Results

Our finding that ErbB2 colocalized with PLAP soon after internalization was surprising in the context of earlier work showing that the GEEC pathway is specific for GPI-anchored proteins. One possible explanation of this discrepancy is that ErbB2 has unusual features that allow it to be internalized by the GEEC pathway, despite exclusion of other transmembrane proteins. To test this idea, a logical next step was to test whether other transmembrane proteins were excluded from the ErbB2-containing vesicles after a short time of internalization. We expressed either PLAP, a chimeric construct composed of the transmembrane and cytosolic portions of VSV G protein fused to PLAP (PLAP-G), or the transmembrane and cytosolic portions of influenza hemaglutinin fused to PLAP (PLAPHA) (Figure 14) in SKBr3 cells. Cross linking affects the distribution of GPI-anchored proteins and causes them to become concentrated in caveolae (Mayor *et al.*, 1994). To avoid any possible antibody-induced cross linking, we generated Alexa-Fluor 488 labeled anti-PLAP Fab fragments to follow PLAP internalization. Fl-Anti ErbB2 antibodies and Alexa-Fluor 488-PLAP Fabs were bound to GA treated cells for 1 hour and cells were then warmed for 5 minutes.

As we had seen earlier, we saw strong colocalization between PLAP and ErbB2 (Figure 15A). PLAP- and ErbB2-positive structures were easily visible along the edges, near the plasma membrane of the cell. When we compared the localization of ErbB2 and the PLAP fusion proteins, we were surprised to see the same degree of colocalization.

Although transmembrane proteins were excluded from the GEEC pathway in CHO cells (Sabharanjak *et al.*, 2002) a GPI-anchored protein and a transmembrane protein were reported to be internalized together by the same clathrin-independent endocytic pathway in Hela cells (Naslavsky *et al.*, 2003). Kalia et al. (2006) suggested that this difference might reflect cell-type specific factors. To test this idea, we co-expressed ErbB2 with PLAP, PLAP-G, or PLAP-HA in CHO cells. ErbB2 internalization is normally very asynchronous in SKBr3 cells with only a small fraction of cells showing uptake after 2-5 minutes of internalization. In contrast, ErbB2, PLAP, PLAP-G, and PLAP-HA internalization was much more robust in CHO cells, with a larger fraction of cells showing internalization at early times. Despite this difference, we were able to visualize internalized ErbB2 and the PLAP proteins easily in both cell types. As in SKBr3 cells, we again found that ErbB2 colocalized with PLAP, PLAP-G, and PLAP-HA to the same degree in CHO cells. We quantified the degree of overlap by colocalization analysis. Confocal images of at least 10 cells were taken and the images processed in ImageJ, as described in Materials and Methods. First, we

validated our colocalization procedure on images with high or low amounts of overlap to determine the maximum and minimum Manders coefficients from our software. We obtained Manders coefficients between 0.65-0.85 for high colocalization, and between 0.10-0.25 for conditions with low colocalization (Figure 17). The average Manders coefficient for ErbB2 overlapping PLAP, PLAP-G, and PLAP-HA, or vice versa, is shown in Figure 18. We saw Manders coefficients approaching 0.7-0.8 for all conditions. Manders coefficient M1 and M2 (see Figure 18 legend) were approximately equal indicating that Similar degree of ErbB2 or PLAP/PLAP chimera internalized in each case.

Our results contradict an earlier report (Sabharanjak *et al.*, 2002) and suggest that even in CHO cells, the GEEC pathway is not specific for GPI-anchored proteins. Instead, other transmembrane proteins, not expected to have unique signals, can also be internalized through this pathway. To provide further support for this conclusion, we checked for colocalization of PLAP, PLAP-G, and PLAP-HA with another GPI-anchored protein, Thy-1. As expected, we saw a nearly complete colocalization with PLAP and Thy-1. Thy-1 also colocalized to the same degree with both PLAP-G and PLAP-HA (Figure 19). Colocalization analysis revealed that the Manders coefficients were between 0.6-0.7 approaching the expected maximum for each condition.

Discussion

Data here provide evidence that GPI-anchored proteins and transmembrane proteins can be internalized by the same endocytic pathway in SKBr3 and CHO cells. This observation contradicted an earlier report that transmembrane proteins were not internalized with GPI-anchored proteins. Although the reasons for this discrepancy are not clear at this time, one possibility will be discussed next.

Our work differed from the other study in the specific endocytic cargo molecules examined. In their 2002 report, Sabbharanjak et al. examined endocytosis of two GPI-anchored proteins: the folate receptor and decay accelerating factor (CD59) (Sabharanjak *et al.*, 2002). They compared the localization of these GPI-anchored proteins to an isoform of folate receptor containing the transmembrane segment of the mouse Fc receptor fused to the cytoplasmic portion of the LDL receptor (FR-TM), the transferrin receptor, a truncated form of the transferrin receptor that did not contain a clathrin localization signal, and N-[N-(7-nitro-2,1,3-benzoxadiazol-4-yl)-ε-aminohexanoyl]-sphingosylphosphorylcholine (C_6-NBD-SM), an exogenously introduced, fluorescently labeled lipid. FR-TM contained a clathrin localization sequence and thus was expected to colocalize with Tf. As expected, they saw little colocalization of folate receptor and CD59 with Tf (colocalization index

~0.25-0.35). (C_6-NBD-SM) also colocalized with Tf (~0.75), but did not colocalize with the folate receptor (~0.3). The truncated transferrin receptor colocalized with C_6-NBD-SM. They argued that since C_6-NBD-SM did not colocalize with the GPI- anchored proteins, but did colocalize with the truncated transferrin receptor, that internalization into GEECs is specific for GPI-anchored proteins. They concluded that the lack of clathrin-pathway sorting motifs from transmembrane proteins, or the absence of a transmembrane sequence altogether, is not sufficient to target proteins and lipids for internalization together with GPI-anchored proteins. It must be noted that the observation that these authors base their conclusions on is indirect. Comparing the localization of the GPI-anchored proteins directly to the truncated transferrin receptor would have been a more direct control for this experiment.

Contrary to results reported by Sabharranjak et al., our results in this section suggest that internalization of GPI-anchored proteins does not occur by a specific, dedicated pathway. We directly compared the localization of GPI-anchored proteins to transmembrane proteins lacking clathrin sorting signals and saw strong colocalization in each case. This supports a scenario whereby internalization of GPI-anchored proteins, ErbB2, and other transmembrane proteins lacking cytoplasmic sorting clathrin sorting motifs are internalized through a constitutive, unregulated endocytic pathway. More work needs to be done to further resolve the conflicts between our data and reports in the literature.

For instance we need to continue the colocalization experiments and compare the localization of Tf to PLAP, PLAP-G and PLAP-HA. It would also be helpful to compare internalization of other GPI-anchored proteins to determine if they behave in the same manner, and thus whether endocytosis through this pathway is a general feature of GPI-anchored proteins.

Experiments in this chapter have only looked at the initial internalization step to determine whether these proteins are internalized by this mechanism into GEECs. It is now clear that while multiple types of cargoes are internalized through this pathway they often have distinct cellular destinations. ErbB2 probably passively recycles in resting cells, but GA treatment redirects the protein to lysosomes for degradation. One report found that this pathway is the major route of entry for cholera toxin in at least once cell type, and this toxin is delivered to the Golgi apparatus (Lencer and Tsai, 2003; Kirkham and Parton, 2005). GPI-anchored proteins merge with clathrin cargoes when they pass through early endosomes, are delivered to the recycling endosome, and ultimately returned to the cell surface. It would be beneficial to further characterize trafficking of PLAP-G and PLAP-HA to determine their final destination. Since very little is known about how this pathway is regulated and the mechanism of internalization has not yet been revealed, further characterizing cargos of this pathway and their trafficking behavior will provide valuable tools for future research.

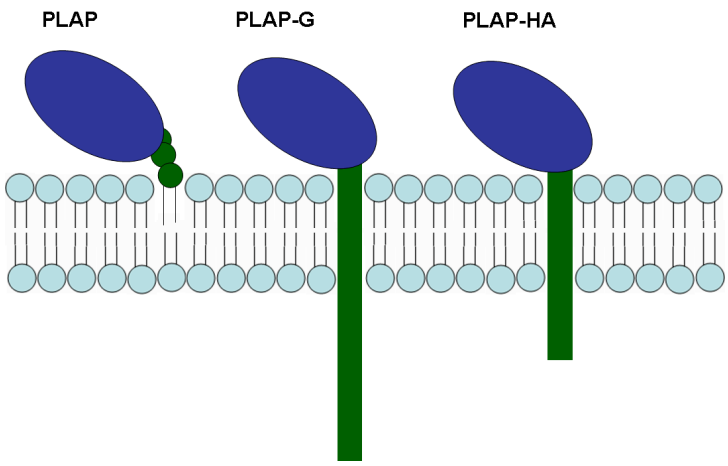

Figure 14. Schematic diagram of PLAP, PLAP-G and PLAP-HA in the membrane. PLAP is represented in blue. For PLAP-G the ectodomain of PLAP was fused in frame to the transmembrane and cytosolic portions of VSV-G protein. For PLAP-HA the transmembrane and cytosolic domains of influenza hemagglutinin were fused in frame to the ectodomain of PLAP**.**

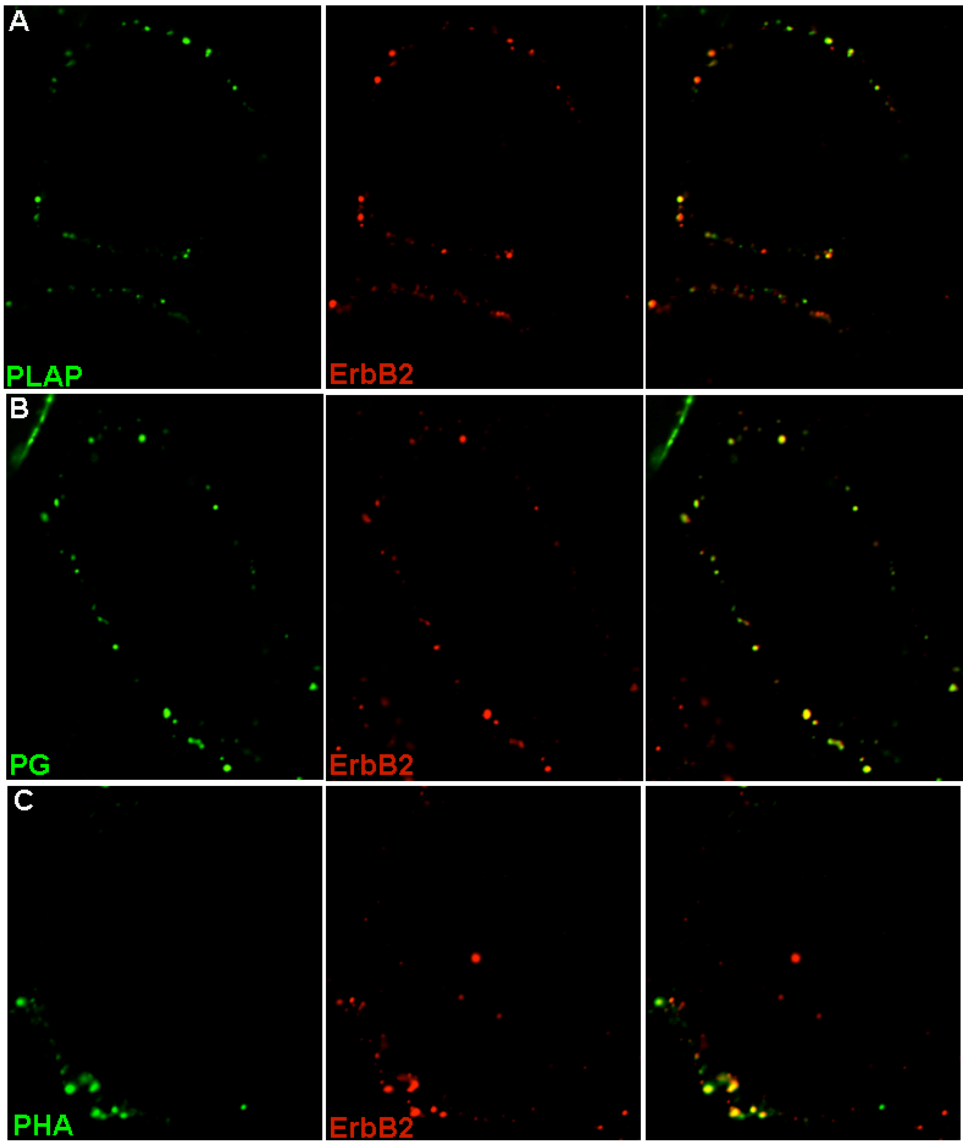

Figure 15. Localization of ErbB2 and PLAP, PLAP-G, or PLAP-HA in SKBr3 cells. SKBr3 cells were transfected with PLAP, PLAP-G (PG), or PLAP-HA (PHA) and examined 36 hours after transfection. Fl-anti-ErbB2 antibodies and rabbit FITC-anti-PLAP Fabs were bound for 1 hour in the cold, cells were warmed for 2 minutes, and residual surface bound antibody removed by acid stripping. The cell were then fixed and examined by deconvolution microscopy. PLAP proteins are on left, ErbB2 is in Middle. Merged images are on the right. PLAP is shown in row A, PLAP-G in row B, and PLAP-HA in row C**.**

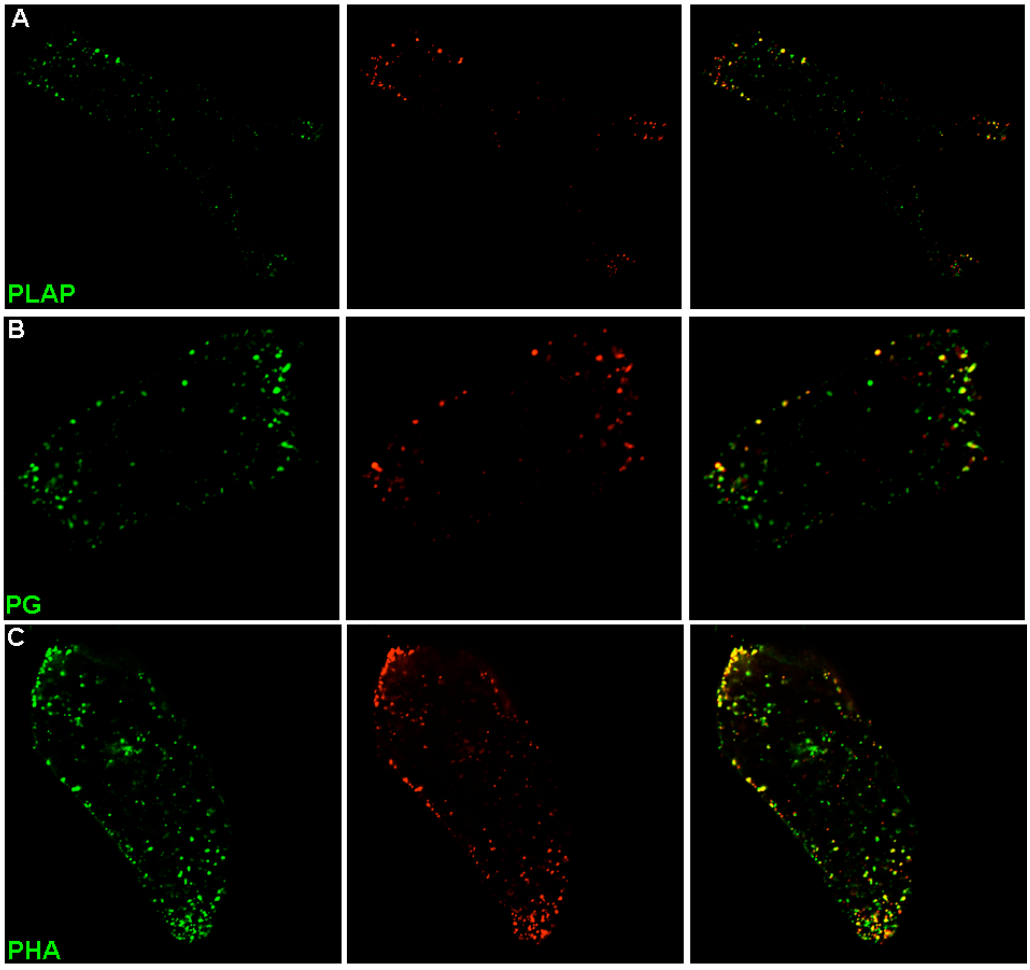

Figure 16. Localization of ErbB2 and PLAP, PLAP-G, or PLAP-HA in CHO cells. CHO cells were co-transfected with ErbB2 and PLAP, PLAP-G (PG), or PLAP-HA (PHA) and examined 24-36 hours after transfection. Fl-anti-ErbB2 antibodies and Rabbit FITC-anti-PLAP Fabs were bound for 1 hour in the cold, cells were warmed for 2 minutes, and residual surface bound antibodies removed by acid stripping. The cell were then fixed and examined by deconvolution microscopy. PLAP proteins are on left, ErbB2 is in Middle, and merged images are on the right. PLAP is shown in row A, PLAP-G in row B, and PLAP-HA in row C**.**

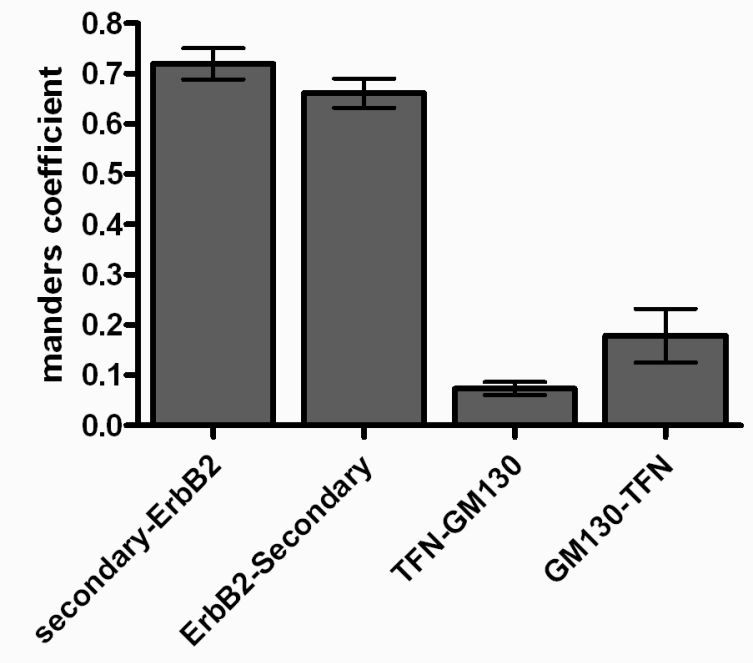

Figure 17. Expected maximum and minimum colocalization. To determine Manders values for maximal colocalization a slide with expected complete colocalization was set up. Cells were pretreated with 5 μM GA for 1 hour, fl-anti-ErbB2 bound for 1 hour in the cold, and the cells warmed for 1 hour. Residual surface bound antibody was removed by acid stripping and the cells were fixed, permeabilized, and Fl-anti-ErbB2 detected with Texas red labeled anti-mouse antibody. For expected low colocalization, cells were pulsed with Alexa-594 Tf for 5 minutes, acid stripped, fixed, permeabilized and the golgi detected with an anti-GM130 antibody and FITC labeled anti mouse antibodies. Images were acquired by confocal microscopy and colocalization analysis performed as described in the method and materials chapter. Maximum values for Manders colocalization coefficients are 1 (perfect overlap), minimum is 0 (complete exclusion). Manders coefficients can be directly interpreted as percentages (for example, .8=80%).

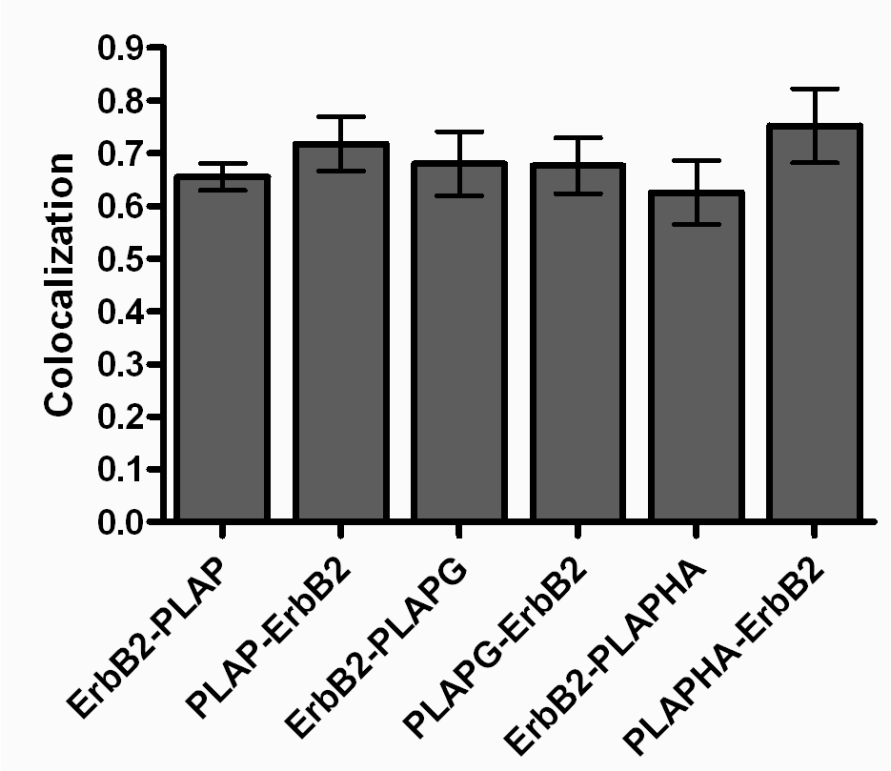

Figure 18. ErbB2 colocalizes with PLAP, PLAPG, and PLAPHA in CHO cells. CHO cells were cotransfected with ErbB2 and PLAP, PLAPG or PLAPHA. Alexa 594 labeled anti-ErbB2 and FITC-labeled PLAP Fabs were bound for 1 hour on ice, and then warmed for 2 minutes. Residual surface bound antibodies were was removed with acid. Cells were imaged by deconvolution microscopy and colocalization measured in imageJ and described in Materials and Methods. Manders coefficients M1 (ErbB2 colocalized with PLAP, PLAPG, or PLAPHA) and M2 (PLAP, PLAPG, or PLAPHA colocalized with ErbB2) are shown. Bars are average of at least 10 cells. Error bars are S.E.M

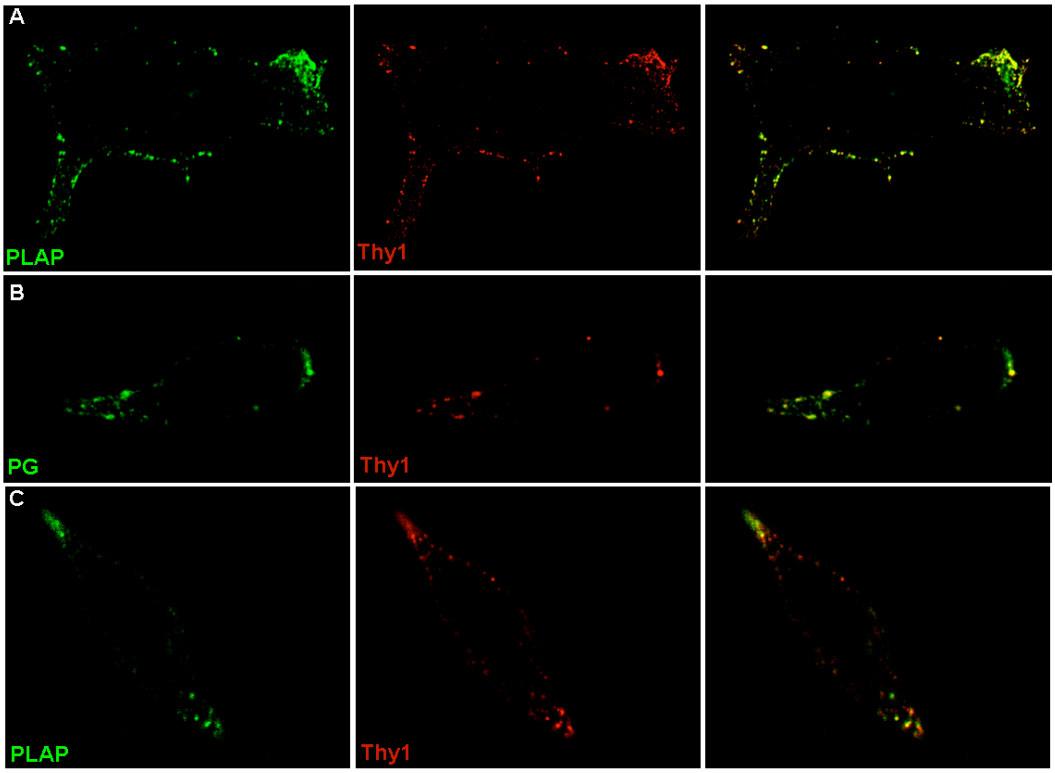

Figure 19. Localization of Thy1 and PLAP, PLAP-G, or PLAP-HA in CHO cells. CHO cells were co-transfected with Thy1 and PLAP, PLAP-G (PG), or PLAP-HA (PHA) and examined 24-36 hours after transfection. Alexa 594 mouse anti-thy1 Fabs and Alexa 488Fluor mouse anti-PLAP Fabs were bound for 1 hour in the cold, warmed for 2 minutes, and residual surface bound antibody removed by acid stripping. The cell were then fixed and examined by deconvolution microscopy. PLAP proteins are shown on left, Thy1 in the middle column. Merged images on the left. PLAP is shown in row A, PLAP-G in row B, and PLAP-HA in row C**.**

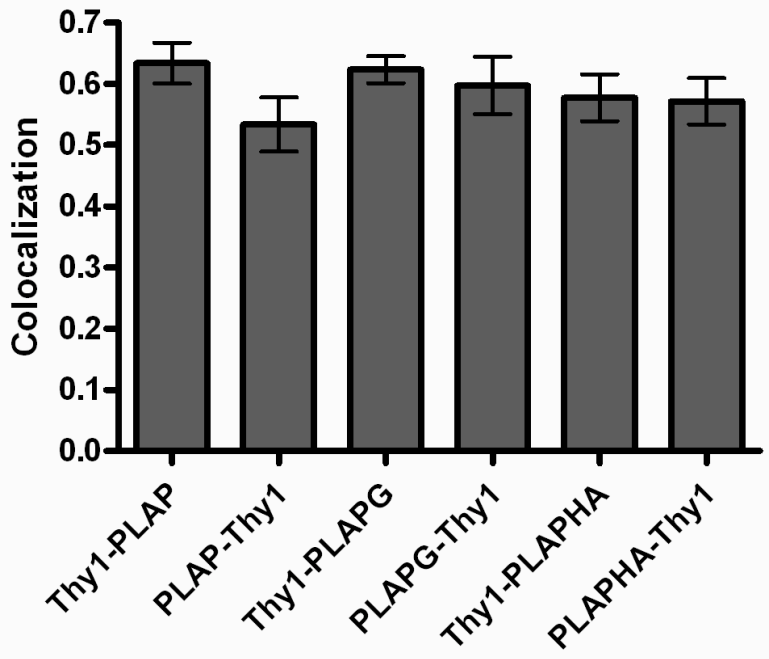

Figure 20. Thy1 colocalizes with PLAP, PLAPG, and PLAPHA in CHO cells. CHO cells were co-transfected with Thy1 and PLAP, PLAPG, or PLAPHA. Alexa Fluor 594 mouse anti-Thy1 and alexa 488 mouse anti-PLAP Fab fragments were bound for 1 hour on ice. The cells were then warmed for 2 minutes, and residual surface antibody removed by acid washing. Cells were imaged by confocal microscopy and colocalization evaluated using imageJ. Bars represent the average of at least 9 cells.

Conclusions

Clathrin-independent pathways represent a rapidly growing field of study. Compared to the well studied clathrin pathway, our knowledge of non-clathrin pathways is still in its infancy. At the present time it is not clear how many clathrin-independent pathways exist, and how these overlap both functionally and mechanistically. The most rapid advancements have been made in identifying new cargoes, and identifying the trafficking characteristics of these cargoes. Events downstream of the initial internalization have been fleshed out in much more detail then the mechanism of internalization itself.

One feature many endocytic pathways seem to share is a convergence on early endosomes. Cargoes for both the GEEC and Arf6 associated pathways are both first taken into vesicles that do not contain markers for early endosomes and are devoid of clathrin cargoes. These vesicles then acquire Rab5 and EEA1 in a process that PI3K kinase, and phosphoinositide conversion on the vesicle membrane. For both pathways inactivation of PI3K blocks delivery of cargoes to early endosomes (Naslavsky *et al.*, 2003; Kalia *et al.*, 2006). Unlike the GEEC pathway, inactivation of Arf6 is also necessary for early endosome transport in the Arf6 associated pathway. The caveolar pathway can also transiently interact with early endosomes. One group saw "shuttling" of caveolar vesicles from the caveosome to early endosomes where cargo was sorted from caveolar domains

(Pelkmans *et al.*, 2004). Convergence on early endosomes appears to be a very important feature of endocytic cargo trafficking.

ErbB2 now provides another marker of a clathrin-independent pathway. Like cargo of the GEEC pathway, it was internalized together with GPI-anchored proteins, cholera toxin, and fluid in GA-treated cells. It behaved similarly in both CHO and SKBr3 cells. Like GEEC cargoes, ErbB2 was internalized into the cell and rapidly merged was early endosomes containing clathrin cargoes. Here ErbB2 diverged from GPI-anchored proteins and was sorted to late endosomes, and lysosomes where it was degraded (Figure 21).

In contrast to a previous report, we found that the GEEC pathway was not specific for GPI-anchored proteins in that ErbB2, and other transmembrane containing proteins that lack clathrin sorting sequences can be internalized by this pathway. This is perhaps not surprising as the pathway appears to operate constitutively, internalizes large amounts of fluid, and many of its cargoes recycle to the plasma membrane. Preliminary work from others in our lab suggests that in transfected COS cells, wild-type ErbB2 is internalized in the same manner as a mutant form of the protein that lacks the cytoplasmic domain, and is thus unable to interact with any cytosolic proteins that might target it specifically for endocytosis. This finding, together with the data presented here, suggest that this pathway represents a bulk internalization pathway where many cargoes can be

internalized including GPI-anchored proteins, transmembrane proteins and extracellular substances.

The lack of regulation and requirements for proteins like dynamin seem to suggest that it is an evolutionarily primitive endocytic pathway compared to the highly regulated clathrin-mediated pathway. It would be interesting to compare non-clathrin pathways in mammalian cells to other taxa to look for similarities. For instance, internalization of both fluid phase markers and GPI-anchored proteins in primary cells derived from *Drosophila* does not require dynamin (Guha *et al.*, 2003).

Considerably more work needs to be done to further define clathrin-independent pathways. The mechanism of internalization needs to be determined. The proteins required for internalization need to be identified and the mechanism of regulation, if any need to be characterized.

Although it is now clear that clathrin- and dynamin-independent pathways represent a major route for internalization in mammalian cells, it is not yet clear how many of these pathways exist, and how they might overlap both functionally, and mechanistically. The current status of the Arf6 associated pathway and the GEEC pathway is a good example of the current deficit in our understanding. While both pathways can internalize similar cargoes, do not require dynamin, are constitutive, and at face value look very similar, cargoes are clearly internalized into an Arf6 regulated endosomal system in HeLa cells, whereas in CHO cells

they are not. It is possible to speculate that the Arf6 and GEEC pathways that are described may actually represent the same pathway. There may be a common core machinery yet to be identified for both pathways, where associated and regulatory proteins may differ between cell type and species. More work on the subject with hopefully tease apart the functional and mechanistic details of these pathways. ErbB2 will provide a valuable tool for such future studies.

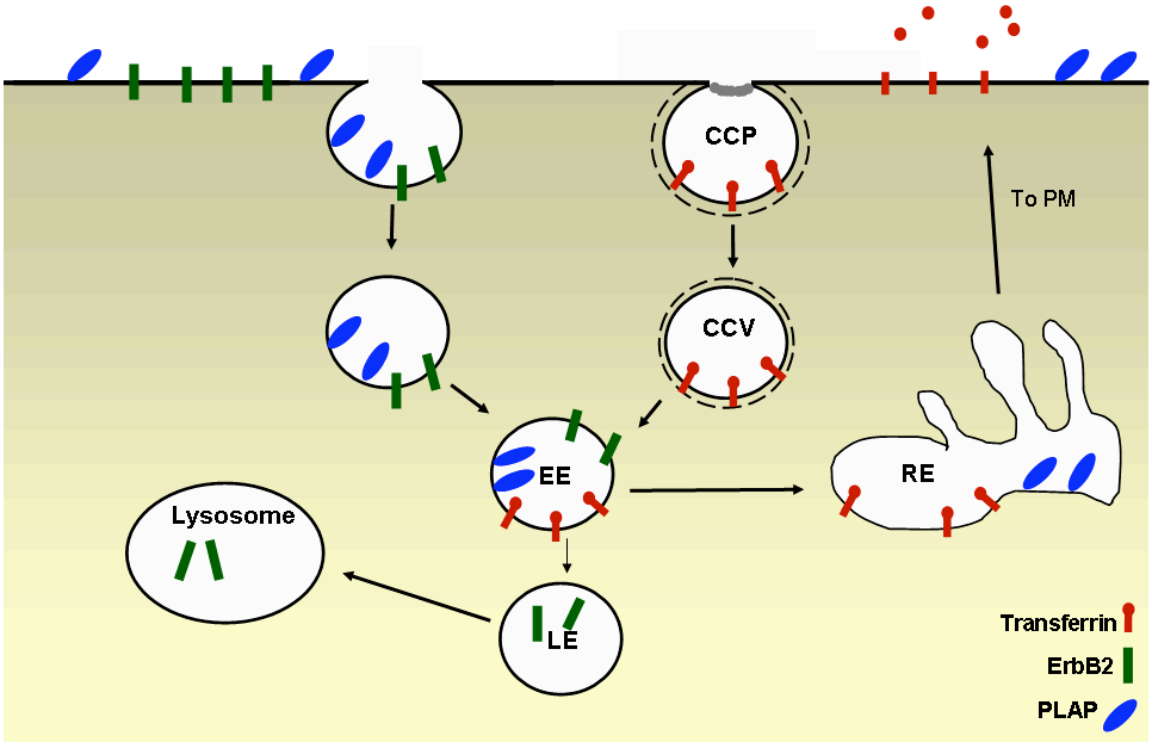

Figure 21. Model for ErbB2 internalization. ErbB2 is internalized with other non-clathrin cargoes by a dynamin and clathrin independent mechanism. Newly internalized ErbB2 is then transported to early endosomes (EE), to late endosomes (LE), and to lysosomes where the receptor is degraded. In contrast GPI-anchored proteins are diverge with ErbB2 in early endosomes and are transported to the recycling endosomes where they are returned to the membrane in a manner similar to cargo internalized by clathrin coated pits (CCP).

Bibliography

Aderem, A., and Underhill, D.M. (1999). Mechanisms of phagocytosis in macrophages. Annu Rev Immunol *17*, 593-623.

Anderson, R.G. (1998). The caveolae membrane system. Annu Rev Biochem *67*, 199-225.

Aridor, M., and Traub, L.M. (2002). Cargo selection in vesicular transport: the making and breaking of a coat. Traffic *3*, 537-546.

Arreaza, G., and Brown, D.A. (1995). Sorting and intracellular trafficking of a glycosylphosphatidylinositol-anchored protein and two hybrid transmembrane proteins with the same ectodomain in Madin-Darby canine kidney epithelial cells. J Biol Chem *270*, 23641-23647.

Arreaza, G., Melkonian, K.A., LaFevre-Bernt, M., and Brown, D.A. (1994). Triton X-100-resistant membrane complexes from cultured kidney epithelial cells contain the Src family protein tyrosine kinase p62yes. J Biol Chem *269*, 19123-19127.

Austin, C.D., De Maziere, A.M., Pisacane, P.I., van Dijk, S.M., Eigenbrot, C., Sliwkowski, M.X., Klumperman, J., and Scheller, R.H. (2004). Endocytosis and sorting of ErbB2 and the site of action of cancer therapeutics trastuzumab and geldanamycin. Mol Biol Cell *15*, 5268-5282.

Austin, C.D., Wen, X., Gazzard, L., Nelson, C., Scheller, R.H., and Scales, S.J. (2005). Oxidizing potential of endosomes and lysosomes limits intracellular cleavage of disulfide-based antibody-drug conjugates. Proc Natl Acad Sci U S A *102*, 17987-17992.

Baulida, J., Kraus, M.H., Alimandi, M., Di Fiore, P.P., and Carpenter, G. (1996). All ErbB receptors other than the epidermal growth factor receptor are endocytosis impaired. J Biol Chem *271*, 5251-5257.

Beerli, R.R., Graus-Porta, D., Woods-Cook, K., Chen, X., Yarden, Y., and Hynes, N.E. (1995). Neu differentiation factor activation of ErbB-3 and ErbB-4 is cell specific and displays a differential requirement for ErbB-2. Mol Cell Biol *15*, 6496-6505.

Benmerah, A., Bayrou, M., Cerf-Bensussan, N., and Dautry-Varsat, A. (1999). Inhibition of clathrin-coated pit assembly by an Eps15 mutant. J Cell Sci *112 (Pt 9)*, 1303-1311.

Berger, J., Howard, A.D., Gerber, L., Cullen, B.R., and Udenfriend, S. (1987). Expression of active, membrane-bound human placental alkaline phosphatase by transfected simian cells. Proc Natl Acad Sci U S A *84*, 4885-4889.

Bolte, S., and Cordelieres, F.P. (2006). A guided tour into subcellular colocalization analysis in light microscopy. J Microsc *224*, 213-232.

Brodsky, F.M., Chen, C.Y., Knuehl, C., Towler, M.C., and Wakeham, D.E. (2001). Biological basket weaving: formation and function of clathrin-coated vesicles. Annu Rev Cell Dev Biol *17*, 517-568.

Burgess, A.W., Cho, H.S., Eigenbrot, C., Ferguson, K.M., Garrett, T.P., Leahy, D.J., Lemmon, M.A., Sliwkowski, M.X., Ward, C.W., and Yokoyama, S. (2003). An open-and-shut case? Recent insights into the activation of EGF/ErbB receptors. Mol Cell *12*, 541-552.

Campanero-Rhodes, M.A., Smith, A., Chai, W., Sonnino, S., Mauri, L., Childs, R.A., Zhang, Y., Ewers, H., Helenius, A., Imberty, A., and Feizi, T. (2007). N-Glycolyl GM1 Ganglioside as a Receptor for Simian Virus 40. J Virol *81*, 12846-12858.

Cardelli, J. (2001). Phagocytosis and macropinocytosis in Dictyostelium: phosphoinositide-based processes, biochemically distinct. Traffic *2*, 311-320.

Citri, A., Alroy, I., Lavi, S., Rubin, C., Xu, W., Grammatikakis, N., Patterson, C., Neckers, L., Fry, D.W., and Yarden, Y. (2002). Drug-induced ubiquitylation and degradation of ErbB receptor tyrosine kinases: implications for cancer therapy. Embo J *21*, 2407-2417.

Citri, A., Gan, J., Mosesson, Y., Vereb, G., Szollosi, J., and Yarden, Y. (2004). Hsp90 restrains ErbB-2/HER2 signalling by limiting heterodimer formation. EMBO Rep *5*, 1165-1170.

Citri, A., Skaria, K.B., and Yarden, Y. (2003). The deaf and the dumb: the biology of ErbB-2 and ErbB-3. Exp Cell Res *284*, 54-65.

Cobleigh, M.A., Vogel, C.L., Tripathy, D., Robert, N.J., Scholl, S., Fehrenbacher, L., Wolter, J.M., Paton, V., Shak, S., Lieberman, G., and Slamon, D.J. (1999). Multinational study of the efficacy and safety of humanized anti-HER2

monoclonal antibody in women who have HER2-overexpressing metastatic breast cancer that has progressed after chemotherapy for metastatic disease. J Clin Oncol *17*, 2639-2648.

Conner, S.D., and Schmid, S.L. (2003). Regulated portals of entry into the cell. Nature *422*, 37-44.

Damke, H., Baba, T., Warnock, D.E., and Schmid, S.L. (1994). Induction of mutant dynamin specifically blocks endocytic coated vesicle formation. J Cell Biol *127*, 915-934.

Damm, E.M., Pelkmans, L., Kartenbeck, J., Mezzacasa, A., Kurzchalia, T., and Helenius, A. (2005). Clathrin- and caveolin-1-independent endocytosis: entry of simian virus 40 into cells devoid of caveolae. J Cell Biol *168*, 477-488.

de Melker, A.A., van der Horst, G., and Borst, J. (2004a). c-Cbl directs EGF receptors into an endocytic pathway that involves the ubiquitin-interacting motif of Eps15. J Cell Sci *117*, 5001-5012.

de Melker, A.A., van der Horst, G., and Borst, J. (2004b). Ubiquitin ligase activity of c-Cbl guides the epidermal growth factor receptor into clathrin-coated pits by two distinct modes of Eps15 recruitment. J Biol Chem *279*, 55465-55473.

Di Guglielmo, G.M., Le Roy, C., Goodfellow, A.F., and Wrana, J.L. (2003). Distinct endocytic pathways regulate TGF-beta receptor signalling and turnover. Nat Cell Biol *5*, 410-421.

Donaldson, J.G. (2003). Multiple roles for Arf6: sorting, structuring, and signaling at the plasma membrane. J Biol Chem *278*, 41573-41576.

Drab, M., Verkade, P., Elger, M., Kasper, M., Lohn, M., Lauterbach, B., Menne, J., Lindschau, C., Mende, F., Luft, F.C., Schedl, A., Haller, H., and Kurzchalia, T.V. (2001). Loss of caveolae, vascular dysfunction, and pulmonary defects in caveolin-1 gene-disrupted mice. Science *293*, 2449-2452.

Duan, L., Miura, Y., Dimri, M., Majumder, B., Dodge, I.L., Reddi, A.L., Ghosh, A., Fernandes, N., Zhou, P., Mullane-Robinson, K., Rao, N., Donoghue, S., Rogers, R.A., Bowtell, D., Naramura, M., Gu, H., Band, V., and Band, H. (2003). Cbl-mediated ubiquitinylation is required for lysosomal sorting of epidermal growth factor receptor but is dispensable for endocytosis. J Biol Chem *278*, 28950-28960.

Dupree, P., Parton, R.G., Raposo, G., Kurzchalia, T.V., and Simons, K. (1993). Caveolae and sorting in the trans-Golgi network of epithelial cells. Embo J *12*, 1597-1605.

Ettenberg, S.A., Keane, M.M., Nau, M.M., Frankel, M., Wang, L.M., Pierce, J.H., and Lipkowitz, S. (1999). cbl-b inhibits epidermal growth factor receptor signaling. Oncogene *18*, 1855-1866.

Fallon, L., Belanger, C.M., Corera, A.T., Kontogiannea, M., Regan-Klapisz, E., Moreau, F., Voortman, J., Haber, M., Rouleau, G., Thorarinsdottir, T., Brice, A., van Bergen En Henegouwen, P.M., and Fon, E.A. (2006). A regulated interaction with the UIM protein Eps15 implicates parkin in EGF receptor trafficking and PI(3)K-Akt signalling. Nat Cell Biol *8*, 834-842.

Fra, A.M., Williamson, E., Simons, K., and Parton, R.G. (1995). De novo formation of caveolae in lymphocytes by expression of VIP21-caveolin. Proc Natl Acad Sci U S A *92*, 8655-8659.

Frank, S.R., Hatfield, J.C., and Casanova, J.E. (1998). Remodeling of the actin cytoskeleton is coordinately regulated by protein kinase C and the ADP-ribosylation factor nucleotide exchange factor ARNO. Mol Biol Cell *9*, 3133-3146.

Fukazawa, T., Miyake, S., Band, V., and Band, H. (1996). Tyrosine phosphorylation of Cbl upon epidermal growth factor (EGF) stimulation and its association with EGF receptor and downstream signaling proteins. J Biol Chem *271*, 14554-14559.

Galbiati, F., Engelman, J.A., Volonte, D., Zhang, X.L., Minetti, C., Li, M., Hou, H., Jr., Kneitz, B., Edelmann, W., and Lisanti, M.P. (2001). Caveolin-3 null mice show a loss of caveolae, changes in the microdomain distribution of the dystrophin-glycoprotein complex, and t-tubule abnormalities. J Biol Chem *276*, 21425-21433.

Galisteo, M.L., Dikic, I., Batzer, A.G., Langdon, W.Y., and Schlessinger, J. (1995). Tyrosine phosphorylation of the c-cbl proto-oncogene protein product and association with epidermal growth factor (EGF) receptor upon EGF stimulation. J Biol Chem *270*, 20242-20245.

Garrett, T.P., McKern, N.M., Lou, M., Elleman, T.C., Adams, T.E., Lovrecz, G.O., Kofler, M., Jorissen, R.N., Nice, E.C., Burgess, A.W., and Ward, C.W.

(2003). The crystal structure of a truncated ErbB2 ectodomain reveals an active conformation, poised to interact with other ErbB receptors. Mol Cell *11*, 495-505.

Guha, A., Sriram, V., Krishnan, K.S., and Mayor, S. (2003). Shibire mutations reveal distinct dynamin-independent and -dependent endocytic pathways in primary cultures of Drosophila hemocytes. J Cell Sci *116*, 3373-3386.

Guignot, J., Caron, E., Beuzon, C., Bucci, C., Kagan, J., Roy, C., and Holden, D.W. (2004). Microtubule motors control membrane dynamics of Salmonella-containing vacuoles. J Cell Sci *117*, 1033-1045.

Haglund, K., Sigismund, S., Polo, S., Szymkiewicz, I., Di Fiore, P.P., and Dikic, I. (2003). Multiple monoubiquitination of RTKs is sufficient for their endocytosis and degradation. Nat Cell Biol *5*, 461-466.

Haslekas, C., Breen, K., Pedersen, K.W., Johannessen, L.E., Stang, E., and Madshus, I.H. (2005). The inhibitory effect of ErbB2 on epidermal growth factor-induced formation of clathrin-coated pits correlates with retention of epidermal growth factor receptor-ErbB2 oligomeric complexes at the plasma membrane. Mol Biol Cell *16*, 5832-5842.

Henley, J.R., Krueger, E.W., Oswald, B.J., and McNiven, M.A. (1998). Dynamin-mediated internalization of caveolae. J Cell Biol *141*, 85-99.

Hernandez-Deviez, D.J., Roth, M.G., Casanova, J.E., and Wilson, J.M. (2004). ARNO and ARF6 regulate axonal elongation and branching through downstream activation of phosphatidylinositol 4-phosphate 5-kinase alpha. Mol Biol Cell *15*, 111-120.

Hinrichsen, L., Harborth, J., Andrees, L., Weber, K., and Ungewickell, E.J. (2003). Effect of clathrin heavy chain- and alpha-adaptin-specific small inhibitory RNAs on endocytic accessory proteins and receptor trafficking in HeLa cells. J Biol Chem *278*, 45160-45170.

Hinshaw, J.E., and Schmid, S.L. (1995). Dynamin self-assembles into rings suggesting a mechanism for coated vesicle budding. Nature *374*, 190-192.

Hohfeld, J., Cyr, D.M., and Patterson, C. (2001). From the cradle to the grave: molecular chaperones that may choose between folding and degradation. EMBO Rep *2*, 885-890.

Hommelgaard, A.M., Lerdrup, M., and van Deurs, B. (2004). Association with membrane protrusions makes ErbB2 an internalization-resistant receptor. Mol Biol Cell *15*, 1557-1567.

Huang, F., Kirkpatrick, D., Jiang, X., Gygi, S., and Sorkin, A. (2006). Differential regulation of EGF receptor internalization and degradation by multiubiquitination within the kinase domain. Mol Cell *21*, 737-748.

Hueffer, K., and Galan, J.E. (2004). Salmonella-induced macrophage death: multiple mechanisms, different outcomes. Cell Microbiol *6*, 1019-1025.

Jiang, X., Huang, F., Marusyk, A., and Sorkin, A. (2003). Grb2 regulates internalization of EGF receptors through clathrin-coated pits. Mol Biol Cell *14*, 858-870.

Jiang, X., and Sorkin, A. (2003). Epidermal growth factor receptor internalization through clathrin-coated pits requires Cbl RING finger and proline-rich domains but not receptor polyubiquitylation. Traffic *4*, 529-543.

Kalia, M., Kumari, S., Chadda, R., Hill, M.M., Parton, R.G., and Mayor, S. (2006). Arf6-independent GPI-anchored protein-enriched early endosomal compartments fuse with sorting endosomes via a Rab5/phosphatidylinositol-3'-kinase-dependent machinery. Mol Biol Cell *17*, 3689-3704.

King, C.R., Borrello, I., Bellot, F., Comoglio, P., and Schlessinger, J. (1988). Egf binding to its receptor triggers a rapid tyrosine phosphorylation of the erbB-2 protein in the mammary tumor cell line SK-BR-3. Embo J *7*, 1647-1651.

Kirchhausen, T. (1999). Adaptors for clathrin-mediated traffic. Annu Rev Cell Dev Biol *15*, 705-732.

Kirkham, M., Fujita, A., Chadda, R., Nixon, S.J., Kurzchalia, T.V., Sharma, D.K., Pagano, R.E., Hancock, J.F., Mayor, S., and Parton, R.G. (2005). Ultrastructural identification of uncoated caveolin-independent early endocytic vehicles. J Cell Biol *168*, 465-476.

Kirkham, M., and Parton, R.G. (2005). Clathrin-independent endocytosis: new insights into caveolae and non-caveolar lipid raft carriers. Biochim Biophys Acta *1745*, 273-286.

Kurzchalia, T.V., and Parton, R.G. (1999). Membrane microdomains and caveolae. Curr Opin Cell Biol *11*, 424-431.

Lamaze, C., Dujeancourt, A., Baba, T., Lo, C.G., Benmerah, A., and Dautry-Varsat, A. (2001). Interleukin 2 receptors and detergent-resistant membrane domains define a clathrin-independent endocytic pathway. Mol Cell *7*, 661-671.

Lange, Y., and Steck, T.L. (1984). Mechanism of red blood cell acanthocytosis and echinocytosis in vivo. J Membr Biol *77*, 153-159.

Lencer, W.I., and Saslowsky, D. (2005). Raft trafficking of AB5 subunit bacterial toxins. Biochim Biophys Acta *1746*, 314-321.

Lencer, W.I., and Tsai, B. (2003). The intracellular voyage of cholera toxin: going retro. Trends Biochem Sci *28*, 639-645.

Lenferink, A.E., Pinkas-Kramarski, R., van de Poll, M.L., van Vugt, M.J., Klapper, L.N., Tzahar, E., Waterman, H., Sela, M., van Zoelen, E.J., and Yarden, Y. (1998). Differential endocytic routing of homo- and hetero-dimeric ErbB tyrosine kinases confers signaling superiority to receptor heterodimers. Embo J *17*, 3385-3397.

Lerdrup, M., Hommelgaard, A.M., Grandal, M., and van Deurs, B. (2006). Geldanamycin stimulates internalization of ErbB2 in a proteasome-dependent way. J Cell Sci *119*, 85-95.

Levkowitz, G., Klapper, L.N., Tzahar, E., Freywald, A., Sela, M., and Yarden, Y. (1996). Coupling of the c-Cbl protooncogene product to ErbB-1/EGF-receptor but not to other ErbB proteins. Oncogene *12*, 1117-1125.

Levkowitz, G., Waterman, H., Ettenberg, S.A., Katz, M., Tsygankov, A.Y., Alroy, I., Lavi, S., Iwai, K., Reiss, Y., Ciechanover, A., Lipkowitz, S., and Yarden, Y. (1999). Ubiquitin ligase activity and tyrosine phosphorylation underlie suppression of growth factor signaling by c-Cbl/Sli-1. Mol Cell *4*, 1029-1040.

Lidke, D.S., and Arndt-Jovin, D.J. (2004). Imaging takes a quantum leap. Physiology (Bethesda) *19*, 322-325.

Lund, K.A., Opresko, L.K., Starbuck, C., Walsh, B.J., and Wiley, H.S. (1990). Quantitative analysis of the endocytic system involved in hormone-induced receptor internalization. J Biol Chem *265*, 15713-15723.

Massol, R.H., Larsen, J.E., Fujinaga, Y., Lencer, W.I., and Kirchhausen, T. (2004). Cholera toxin toxicity does not require functional Arf6- and dynamin-dependent endocytic pathways. Mol Biol Cell *15*, 3631-3641.

Maxfield, F.R., and McGraw, T.E. (2004). Endocytic recycling. Nat Rev Mol Cell Biol *5*, 121-132.

Mayor, S., and Pagano, R.E. (2007). Pathways of clathrin-independent endocytosis. Nat Rev Mol Cell Biol *8*, 603-612.

Mayor, S., Rothberg, K.G., and Maxfield, F.R. (1994). Sequestration of GPI-anchored proteins in caveolae triggered by cross-linking. Science *264*, 1948-1951.

Meier, O., Boucke, K., Hammer, S.V., Keller, S., Stidwill, R.P., Hemmi, S., and Greber, U.F. (2002). Adenovirus triggers macropinocytosis and endosomal leakage together with its clathrin-mediated uptake. J Cell Biol *158*, 1119-1131.

Meisner, H., and Czech, M.P. (1995). Coupling of the proto-oncogene product c-Cbl to the epidermal growth factor receptor. J Biol Chem *270*, 25332-25335.

Mellman, I. (1996). Membranes and sorting. Curr Opin Cell Biol *8*, 497-498.

Mellman, I., and Steinman, R.M. (2001). Dendritic cells: specialized and regulated antigen processing machines. Cell *106*, 255-258.

Mimnaugh, E.G., Chavany, C., and Neckers, L. (1996). Polyubiquitination and proteasomal degradation of the p185c-erbB-2 receptor protein-tyrosine kinase induced by geldanamycin. J Biol Chem *271*, 22796-22801.

Minshall, R.D., Tiruppathi, C., Vogel, S.M., Niles, W.D., Gilchrist, A., Hamm, H.E., and Malik, A.B. (2000). Endothelial cell-surface gp60 activates vesicle formation and trafficking via G(i)-coupled Src kinase signaling pathway. J Cell Biol *150*, 1057-1070.

Monier, S., Parton, R.G., Vogel, F., Behlke, J., Henske, A., and Kurzchalia, T.V. (1995). VIP21-caveolin, a membrane protein constituent of the caveolar coat, oligomerizes in vivo and in vitro. Mol Biol Cell *6*, 911-927.

Motley, A., Bright, N.A., Seaman, M.N., and Robinson, M.S. (2003). Clathrin-mediated endocytosis in AP-2-depleted cells. J Cell Biol *162*, 909-918.

Muthuswamy, S.K., Gilman, M., and Brugge, J.S. (1999). Controlled dimerization of ErbB receptors provides evidence for differential signaling by homo- and heterodimers. Mol Cell Biol *19*, 6845-6857.

Nagy, P., Vereb, G., Sebestyen, Z., Horvath, G., Lockett, S.J., Damjanovich, S., Park, J.W., Jovin, T.M., and Szollosi, J. (2002). Lipid rafts and the local density

of ErbB proteins influence the biological role of homo- and heteroassociations of ErbB2. J Cell Sci *115*, 4251-4262.

Naslavsky, N., Weigert, R., and Donaldson, J.G. (2003). Convergence of non-clathrin- and clathrin-derived endosomes involves Arf6 inactivation and changes in phosphoinositides. Mol Biol Cell *14*, 417-431.

Naslavsky, N., Weigert, R., and Donaldson, J.G. (2004). Characterization of a nonclathrin endocytic pathway: membrane cargo and lipid requirements. Mol Biol Cell *15*, 3542-3552.

Ostermeyer, A.G., Paci, J.M., Zeng, Y., Lublin, D.M., Munro, S., and Brown, D.A. (2001). Accumulation of caveolin in the endoplasmic reticulum redirects the protein to lipid storage droplets. J Cell Biol *152*, 1071-1078.

Ostermeyer, A.G., Ramcharan, L.T., Zeng, Y., Lublin, D.M., and Brown, D.A. (2004). Role of the hydrophobic domain in targeting caveolin-1 to lipid droplets. J Cell Biol *164*, 69-78.

Parton, R.G., Joggerst, B., and Simons, K. (1994). Regulated internalization of caveolae. J Cell Biol *127*, 1199-1215.

Parton, R.G., and Simons, K. (2007). The multiple faces of caveolae. Nat Rev Mol Cell Biol *8*, 185-194.

Pelkmans, L. (2005). Viruses as probes for systems analysis of cellular signalling, cytoskeleton reorganization and endocytosis. Curr Opin Microbiol *8*, 331-337.

Pelkmans, L., Burli, T., Zerial, M., and Helenius, A. (2004). Caveolin-stabilized membrane domains as multifunctional transport and sorting devices in endocytic membrane traffic. Cell *118*, 767-780.

Pelkmans, L., and Helenius, A. (2002). Endocytosis via caveolae. Traffic *3*, 311-320.

Pelkmans, L., Kartenbeck, J., and Helenius, A. (2001). Caveolar endocytosis of simian virus 40 reveals a new two-step vesicular-transport pathway to the ER. Nat Cell Biol *3*, 473-483.

Pelkmans, L., Puntener, D., and Helenius, A. (2002). Local actin polymerization and dynamin recruitment in SV40-induced internalization of caveolae. Science *296*, 535-539.

Razani, B., Engelman, J.A., Wang, X.B., Schubert, W., Zhang, X.L., Marks, C.B., Macaluso, F., Russell, R.G., Li, M., Pestell, R.G., Di Vizio, D., Hou, H., Jr., Kneitz, B., Lagaud, G., Christ, G.J., Edelmann, W., and Lisanti, M.P. (2001). Caveolin-1 null mice are viable but show evidence of hyperproliferative and vascular abnormalities. J Biol Chem *276*, 38121-38138.

Razani, B., Woodman, S.E., and Lisanti, M.P. (2002). Caveolae: from cell biology to animal physiology. Pharmacol Rev *54*, 431-467.

Richter, K., and Buchner, J. (2001). Hsp90: chaperoning signal transduction. J Cell Physiol *188*, 281-290.

Ridley, A.J. (2001). Rho proteins: linking signaling with membrane trafficking. Traffic *2*, 303-310.

Roskoski, R., Jr. (2004). The ErbB/HER receptor protein-tyrosine kinases and cancer. Biochem Biophys Res Commun *319*, 1-11.

Rothberg, K.G., Heuser, J.E., Donzell, W.C., Ying, Y.S., Glenney, J.R., and Anderson, R.G. (1992). Caveolin, a protein component of caveolae membrane coats. Cell *68*, 673-682.

Rowinsky, E.K. (2004). The erbB family: targets for therapeutic development against cancer and therapeutic strategies using monoclonal antibodies and tyrosine kinase inhibitors. Annu Rev Med *55*, 433-457.

Sabharanjak, S., Sharma, P., Parton, R.G., and Mayor, S. (2002). GPI-anchored proteins are delivered to recycling endosomes via a distinct cdc42-regulated, clathrin-independent pinocytic pathway. Dev Cell *2*, 411-423.

Schmid, S.L. (1997). Clathrin-coated vesicle formation and protein sorting: an integrated process. Annu Rev Biochem *66*, 511-548.

Schubert, W., Frank, P.G., Razani, B., Park, D.S., Chow, C.W., and Lisanti, M.P. (2001). Caveolae-deficient endothelial cells show defects in the uptake and transport of albumin in vivo. J Biol Chem *276*, 48619-48622.

Sever, S., Damke, H., and Schmid, S.L. (2000). Garrotes, springs, ratchets, and whips: putting dynamin models to the test. Traffic *1*, 385-392.

Sever, S., Muhlberg, A.B., and Schmid, S.L. (1999). Impairment of dynamin's GAP domain stimulates receptor-mediated endocytosis. Nature *398*, 481-486.

Sharma, D.K., Brown, J.C., Choudhury, A., Peterson, T.E., Holicky, E., Marks, D.L., Simari, R., Parton, R.G., and Pagano, R.E. (2004). Selective stimulation of caveolar endocytosis by glycosphingolipids and cholesterol. Mol Biol Cell *15*, 3114-3122.

Sharp, S., and Workman, P. (2006). Inhibitors of the HSP90 molecular chaperone: current status. Adv Cancer Res *95*, 323-348.

Sigismund, S., Woelk, T., Puri, C., Maspero, E., Tacchetti, C., Transidico, P., Di Fiore, P.P., and Polo, S. (2005). Clathrin-independent endocytosis of ubiquitinated cargos. Proc Natl Acad Sci U S A *102*, 2760-2765.

Simpson, F., Bright, N.A., West, M.A., Newman, L.S., Darnell, R.B., and Robinson, M.S. (1996). A novel adaptor-related protein complex. J Cell Biol *133*, 749-760.

Slamon, D.J., Clark, G.M., Wong, S.G., Levin, W.J., Ullrich, A., and McGuire, W.L. (1987). Human breast cancer: correlation of relapse and survival with amplification of the HER-2/neu oncogene. Science *235*, 177-182.

Sorkin, A., Di Fiore, P.P., and Carpenter, G. (1993). The carboxyl terminus of epidermal growth factor receptor/erbB-2 chimerae is internalization impaired. Oncogene *8*, 3021-3028.

Soubeyran, P., Kowanetz, K., Szymkiewicz, I., Langdon, W.Y., and Dikic, I. (2002). Cbl-CIN85-endophilin complex mediates ligand-induced downregulation of EGF receptors. Nature *416*, 183-187.

Stang, E., Blystad, F.D., Kazazic, M., Bertelsen, V., Brodahl, T., Raiborg, C., Stenmark, H., and Madshus, I.H. (2004). Cbl-dependent ubiquitination is required for progression of EGF receptors into clathrin-coated pits. Mol Biol Cell *15*, 3591-3604.

Steele-Mortimer, O., Knodler, L.A., and Finlay, B.B. (2000). Poisons, ruffles and rockets: bacterial pathogens and the host cell cytoskeleton. Traffic *1*, 107-118.

Stenmark, H., Parton, R.G., Steele-Mortimer, O., Lutcke, A., Gruenberg, J., and Zerial, M. (1994). Inhibition of rab5 GTPase activity stimulates membrane fusion in endocytosis. Embo J *13*, 1287-1296.

Stern, D.F., Heffernan, P.A., and Weinberg, R.A. (1986). p185, a product of the neu proto-oncogene, is a receptorlike protein associated with tyrosine kinase activity. Mol Cell Biol *6*, 1729-1740.

Sweitzer, S.M., and Hinshaw, J.E. (1998). Dynamin undergoes a GTP-dependent conformational change causing vesiculation. Cell *93*, 1021-1029.

Tang, Z., Scherer, P.E., Okamoto, T., Song, K., Chu, C., Kohtz, D.S., Nishimoto, I., Lodish, H.F., and Lisanti, M.P. (1996). Molecular cloning of caveolin-3, a novel member of the caveolin gene family expressed predominantly in muscle. J Biol Chem *271*, 2255-2261.

Thomsen, P., Roepstorff, K., Stahlhut, M., and van Deurs, B. (2002). Caveolae are highly immobile plasma membrane microdomains, which are not involved in constitutive endocytic trafficking. Mol Biol Cell *13*, 238-250.

Tikhomirov, O., and Carpenter, G. (2000). Geldanamycin induces ErbB-2 degradation by proteolytic fragmentation. J Biol Chem *275*, 26625-26631.

Tikhomirov, O., and Carpenter, G. (2001). Caspase-dependent cleavage of ErbB-2 by geldanamycin and staurosporin. J Biol Chem *276*, 33675-33680.

Tiruppathi, C., Song, W., Bergenfeldt, M., Sass, P., and Malik, A.B. (1997). Gp60 activation mediates albumin transcytosis in endothelial cells by tyrosine kinase-dependent pathway. J Biol Chem *272*, 25968-25975.

Traub, L.M. (2003). Sorting it out: AP-2 and alternate clathrin adaptors in endocytic cargo selection. J Cell Biol *163*, 203-208.

Volpicelli, L.A., Lah, J.J., and Levey, A.I. (2001). Rab5-dependent trafficking of the m4 muscarinic acetylcholine receptor to the plasma membrane, early endosomes, and multivesicular bodies. J Biol Chem *276*, 47590-47598.

Vonderheit, A., and Helenius, A. (2005). Rab7 associates with early endosomes to mediate sorting and transport of Semliki forest virus to late endosomes. PLoS Biol *3*, e233.

Wadia, J.S., Stan, R.V., and Dowdy, S.F. (2004). Transducible TAT-HA fusogenic peptide enhances escape of TAT-fusion proteins after lipid raft macropinocytosis. Nat Med *10*, 310-315.

Wang, L.H., Rothberg, K.G., and Anderson, R.G. (1993). Mis-assembly of clathrin lattices on endosomes reveals a regulatory switch for coated pit formation. J Cell Biol *123*, 1107-1117.

Wang, Z., and Moran, M.F. (1996). Requirement for the adapter protein GRB2 in EGF receptor endocytosis. Science *272*, 1935-1939.

Wang, Z., Zhang, L., Yeung, T.K., and Chen, X. (1999). Endocytosis deficiency of epidermal growth factor (EGF) receptor-ErbB2 heterodimers in response to EGF stimulation. Mol Biol Cell *10*, 1621-1636.

Waterman, H., Alroy, I., Strano, S., Seger, R., and Yarden, Y. (1999). The C-terminus of the kinase-defective neuregulin receptor ErbB-3 confers mitogenic superiority and dictates endocytic routing. Embo J *18*, 3348-3358.

Way, M., and Parton, R.G. (1995). M-caveolin, a muscle-specific caveolin-related protein. FEBS Lett *376*, 108-112.

Way, T.D., Kao, M.C., and Lin, J.K. (2004). Apigenin induces apoptosis through proteasomal degradation of HER2/neu in HER2/neu-overexpressing breast cancer cells via the phosphatidylinositol 3-kinase/Akt-dependent pathway. J Biol Chem *279*, 4479-4489.

Xu, W., Marcu, M., Yuan, X., Mimnaugh, E., Patterson, C., and Neckers, L. (2002). Chaperone-dependent E3 ubiquitin ligase CHIP mediates a degradative pathway for c-ErbB2/Neu. Proc Natl Acad Sci U S A *99*, 12847-12852.

Xu, W., Mimnaugh, E., Rosser, M.F., Nicchitta, C., Marcu, M., Yarden, Y., and Neckers, L. (2001). Sensitivity of mature Erbb2 to geldanamycin is conferred by its kinase domain and is mediated by the chaperone protein Hsp90. J Biol Chem *276*, 3702-3708.

Xu, W., Yuan, X., Beebe, K., Xiang, Z., and Neckers, L. (2007). Loss of Hsp90 association up-regulates Src-dependent ErbB2 activity. Mol Cell Biol *27*, 220-228.

Yamada, E. (1955). The fine structure of the gall bladder epithelium of the mouse. J Biophys Biochem Cytol *1*, 445-458.

Yang, X.L., Xiong, W.C., and Mei, L. (2004). Lipid rafts in neuregulin signaling at synapses. Life Sci *75*, 2495-2504.

Yarden, Y., and Sliwkowski, M.X. (2001). Untangling the ErbB signalling network. Nat Rev Mol Cell Biol *2*, 127-137.

Zhou, P., Fernandes, N., Dodge, I.L., Reddi, A.L., Rao, N., Safran, H., DiPetrillo, T.A., Wazer, D.E., Band, V., and Band, H. (2003). ErbB2 degradation mediated by the co-chaperone protein CHIP. J Biol Chem *278*, 13829-13837.

Zhou, W., and Carpenter, G. (2001). Heregulin-dependent translocation and hyperphosphorylation of ErbB-2. Oncogene *20*, 3918-3920.

Zurita, A.R., Crespo, P.M., Koritschoner, N.P., and Daniotti, J.L. (2004). Membrane distribution of epidermal growth factor receptors in cells expressing different gangliosides. Eur J Biochem *271*, 2428-2437.